A Measurement of the Value of h/e by the Determination of the Short Wavelength Limit of the Continuous X-ray Spectrum at 20 kV

Thesis by

Wolfgang K. H. Panofsky

In Partial Fulfillment of the Requirements for the

Degree of Doctor of Philosophy

California Institute of Technology

Pasadena, California

1941

Table of Contents

Abstract

In order to investigate the causes of the discrepancy among the measurable functions of the atomic constants ê, h, and m, a redetermination of the ratio $h/\hat{e}$ was undertaken by the method of the determination of the short wavelength limit of the continuous x-ray spectrum. The reliability of the measurements is increased due to

1) The use of large primary intensity

2) Automatic voltage stabilization

3) Improved methods of voltage measurement

4) Improved monochromatization by the combined use of balanced filters and a 2-crystal spectrometer of high resolving power

5) Cleaning of the target in vacuo

The results of the work indicate a value of

$$h/\hat{e} = 1.3786 \times 10^{-17} \text{ erg sec/esu}$$

The sources of error are discussed.

The fundamental atomic constants e, m, and h have in recent years become the source of renewed interest, principally due to the fact that new determinations of various functions of these quantities failed to be mutually consistent within expected limits of error.

The functions of e, m, and h which can be determined with a precision sufficient for consideration here, are:

Function	Method of determinations	References
1) e	absolute X-ray wavelengths	1 - 6
	Oil drop method	7 - 9
2) e/m	Deflection methods	10 - 13
	Zeemann effect	19 - 20
	R_∞/R	14 - 18
	Index of refraction of X-rays	21
3) h/e	Shortwavelength limits of the continuous X-ray spectrum	22 - 31
	Excitation potentials in gases	36 - 55
	Photoelectric effect	33 - 35
	Excitation potentials of X-ray lines	30
4) $\frac{h}{(em)^{1/2}}$	Radiation constant c_2	32
	Electron wavelength vs. electron voltage	56 - 57
5) $\frac{e^4 m}{h^3}$	R_∞	58
6) h/m	Compton shift	59
	Electron wavelength vs. electron velocity	60
7) $\frac{e^2}{h}$	Fine structure constant determination by the separation of X-ray doublets	61
8) $\frac{e}{(mh)^{1/2}}$	Magnetic deflection of X-ray photoelectrons	62
9) $\frac{e^4}{h^3}$	Stefan - Boltzman constant	

Table I

For the details of these methods of determination the reader is referred to the references quoted, or to the general discussion by Birge[65] [66], DuMond[67] [68], Dunnington[69] and Kirchner[70].

The problem of the correlation between experimental results as obtained by the methods named above has been attacked by several authors. Both purely statistical[66] [69] and geometrical[67] [68] methods have been used. By all these different methods of analysis it becomes evident that there seems to exist a considerable disagreement of the various determinations. From these analyses it becomes clear, however, that the h/e determinations play a special role among the measurements considered; all determinations can be brought into fairly satisfactory agreement, provided the h/e determinations are omitted from the considerations. The discrepancy looked so serious at a time that even flaws in the theory underlying the experiments were suggested. The existence of this disagreement was first pointed out by Birge,[71] in particular the special role played by h/e was pointed out by him. At present the situation stands as follows:

If the most probable[66] values of e/m, Avagadro's number N_o, R_∞ and the Faraday are combined, one obtains

$$h/e = \left\{\frac{2\pi^2 c^3 F^2}{R_\infty N_o^2 (e/m)}\right\}^{1/3} = (1.3793 \pm .0002) \times 10^{-17} \text{ erg sec/esu}$$

As compared to this, the values of h/e as measured directly by the shortwavelength limit method are

Duane, Palmer and Yeh[22] $1.3749_4 \times 10^{-17}$ erg sec/esu

Kirkpatrick and Ross (re-computed by DuMond)[23]	$1.3754_1 \times 10^{-17}$ erg sec/esu
Feder (re-computed by DuMond)[24]	$1.3758_8 \times 10^{-17}$
Schaitberger (re-computed by DuMond)[31]	1.3775×10^{-17}
DuMond and Bollman (re-computed by DuMond)[25]	$1.3764_6 \times 10^{-17}$
Bearden and Schwarz[30]	1.3772×10^{-17} and 1.3778×10^{-17}
Ohlin[26] [28] (as corrected by Birge)[72]	1.3800×10^{-17}

Table II

It is seen, therefore, that excepting for the low voltage work of Ohlin[26] [28] all other direct h/e values are from .2% to .3% lower than the indirectly computed one. Due to these large discrepancies a least square solution for a "most probable" value of h/e would be without significance at present. A good view as to the atomic constants situation in general is offered by the "Isometric Consistency Chart" of DuMond[67] [68]. This chart is constructed as follows: Consider the surfaces defined by the function of e, h, and m be plotted on a Cartesion co-ordinate system with e, h, and m as the co-ordinate aces. Let us now take the intersection of these surfaces with the Rydberg - constant surface $\frac{e^4 m}{h^3} \sim$ constant and project these intersecp tions onto a plane normal to the 1, 1, 1 axis of the coordinate system. Since the only values of e, h, and m close to a central value are of interest, the curves will be approximated by straight lines (Fig. I).

Any new determination of the value of h/e must therefore not be undertaken for the purpose of lowering the probable error of an already well established result, but rather for the purpose of discovering hitherto unsuspected sources of error. It is with the latter goal in mind that this re-determination was undertaken.

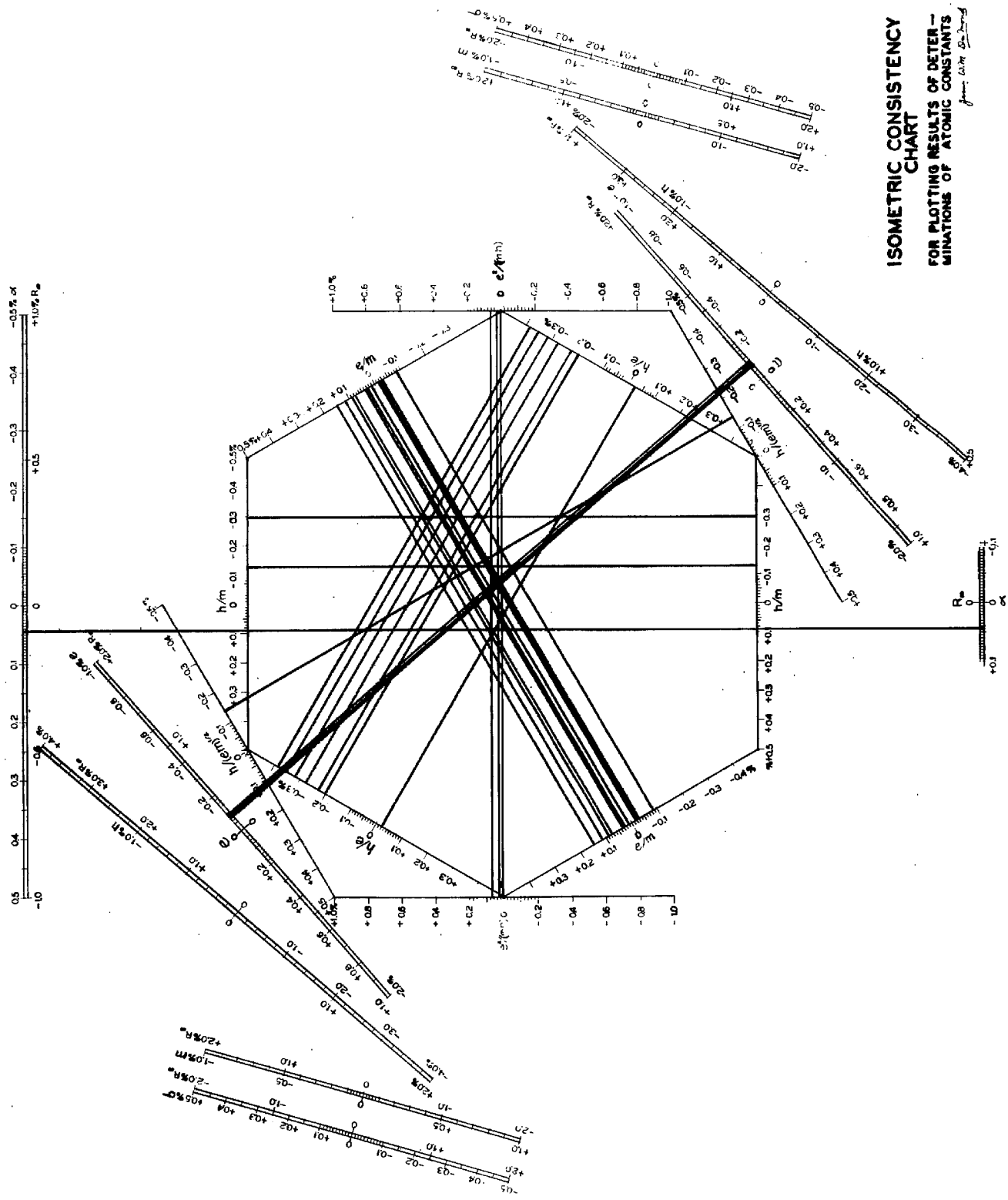
ISOMETRIC CONSISTENCY CHART
FOR PLOTTING RESULTS OF DETERMINATIONS OF ATOMIC CONSTANTS

Fig. I

Figure I Isometric Consistency Chart of the Atomic Constants

The origin of the chart is arbitrarily chosen as

$e_o = 4.80650 \times 10^{-10}$ e.s.u.

$m_o = 9.11780 \times 10^{-28}$ gram

$h_o = 6.63428 \times 10^{-27}$ erg sec

$e_o/m_o = 1.75850 \times 10^{+7}$ e.m.u / gram

$h_o/e_o = 1.38028 \times 10^{-17}$ e.s.u.

$h_o/m_o = 7.27621$ c.g.s.u.

$e_o^2/h_o m_o = 3.81921 \times 10^{24}$ e.s.u.

$h_o/(e_o m_o)^{1/2} = 1.00216 \times 10^{-8}$ e.s.u.

$R_\infty = 109{,}737$ cm^{-1}

$\alpha_o = 7.29870 \times 10^{-3}$

The auxiliary constants used in the values plotted are

$C = 2.99776 \times 10^{10}$ cm/sec

$F = 9651.4$ absolute e.m.u. x (physical gram equivalent)$^{-1}$

$p = 1.00048$

$q = .99986$

$pq = 1.00034$

$\lambda g / \lambda s = 1.00203$

The values plotted are, readinggiin all cases from highest to lowest values:

$e = 4.8030 \times 10^{-10}$	Söderman [5]
4.8026	Bearden [2,3,4,]
4.8021	Bäcklin [1]
$e/m = 1.76110 \times 10^{7}$	Perry and Chaffee [111]
1.76048	Houston and Chu [15-16] [112]
1.76006	Bearden [21]
1.75982	Dunnington [10]
1.75914	C. Robinson [113]
1.75913	Drinkwater, Richardson and Williams [114]

Fig. I Isometric Consistency Chart of the Atomic Constants - B

$e/_m$	1.75900	Kirchner[11-12]
	1.75870	Gaedicke[115]
	1.75820	Shaw[13]
	1.75815	Shawe and Spedding[17]
	1.75797	R. C. Williams[18]
	1.75700	Kinsler and Houston[19]
$h/_e$	1.3800×10^{-17}	Ohlin[26-28]
	1.3775	Schwarz and Bearden[30]
	1.3775	Schaitberger[31]
	1.37646	DuMond and Bollman[35]
	1.3759	Feder[24]
	1.3754	Kirkpatrick & Ross[23]
	1.3749	Duane, Palmer, and Yeh[22]
$\frac{e^2}{mh}$	3.82188×10^{34}	Robinson[62]
	3.8203	Robinson and Clews[63]
	3.8194	Kretschmar[64]
$h/_m$	7.255	Ross and Kirkpatrick[59]
	7.267	Gnan[60]
$1/_\alpha$	136.95	Christy and Keller[61]

The values of e are those calculated by Birge[116], but corrected to correspond to the value of the Faraday given above.

The value of $e/_m$ are those calculated by Birge[58].

The values of $h/_e$ are those re-calculated by DuMond[68], excepting for the value of Ohlin, which is corrected for the cathode workfunction by Birge[72].

The values of $h/_m$ are as corrected by Kirchner[70].

The values of e^2/mh of Robinson were corrected here for the

Fig. I Isometric Consistency Chart of the Atomic Constants - C

changes in auxiliary constants.

The value of e^2/mh of Kretschmar were corrected by Kretschmar.

II The Isochromat Method

1) Definition of an Ideal Isochromat

The method of locating the short wavelength limit of the continuous X-ray spectrum adopted in the present investigation as well as in the past work quoted in the method of "isochromats". This method ideally consists in perfectly monochromatizing an X-ray beam and then measuring the X-ray intensity as a function of a controllable, but perfectly steady, applied X-ray tube voltage. In practice neither a perfectly monochromatic X-ray beam nor an electron beam perfectly homogeneous as to velocity can be realized; therefore the effect of the deviation from the ideal isochromat condition deserves special consideration.

For an ideal isochromat the value of h/e would be given by

$$\frac{h}{e} = \frac{\lambda V_{min} \times 10^8}{c^2} \qquad (1)$$

where λ is the absolute wavelength in cm of the ideally monochromatic beam; V_{min} is the limiting voltage applied to the X-ray tube measured in absolute Volts* below which the X-ray intensity vanishes. In these units h/e will be measured in erg sec/e.s.u.

2) Energy Level Relations in the X-ray Tube Circuit - the Work-function Correction

The quantity V_{min} appearing in eq. (1) is strictly equal to the threshhold voltage applied to the tube only if the energy U of an electron hitting the target when a voltage V is applied across the tube, were given exactly by

$$U = Ve \qquad (2)$$

* By "absolute volts" we mean the unit 10^8 times larger than the e, m, u - c.g.s. unit of potential difference

The voltage V we assume is measured by a voltmeter connected to the target and the filament leads. In order to investigate what the energy of an electron would actually be when hitting the anode let us draw the schematic circuit involved:

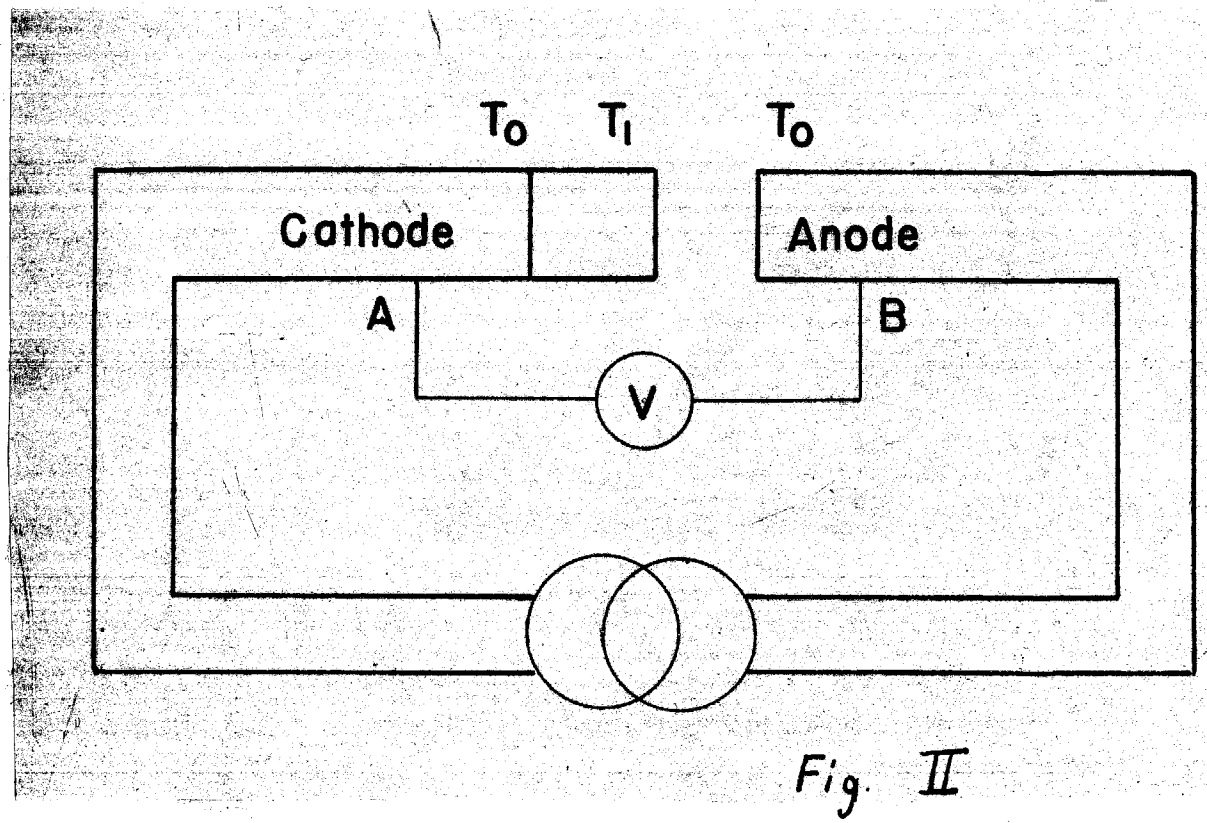

Fig. II

The cathode is at a high temperature T_1; the anode and the filament leads are assumed to be approximately at room temperature T_0.

No current will flow through any conductor provided the edges* of the Fermi electron gas energy distribution are at the same energy values at the two terminals of the conductor. The voltage V measured by the voltmeter as shown corresponds, therefore, to the difference in energy of the edges of the Fermi distribution at A and B. Hence let us draw an energy level diagram of the circuit A-B(Fig. III).

* By the "edge" of the Fermi distribution we mean the mean upper energy limit of the electron distribution; if f (E) d E is the number of electrons within the energy range extending from E to E + d E then the energy corresponding to the "edge" is given by

$$E_e = \frac{\int_0^\infty f(E)\, d\, E}{f(0)}$$

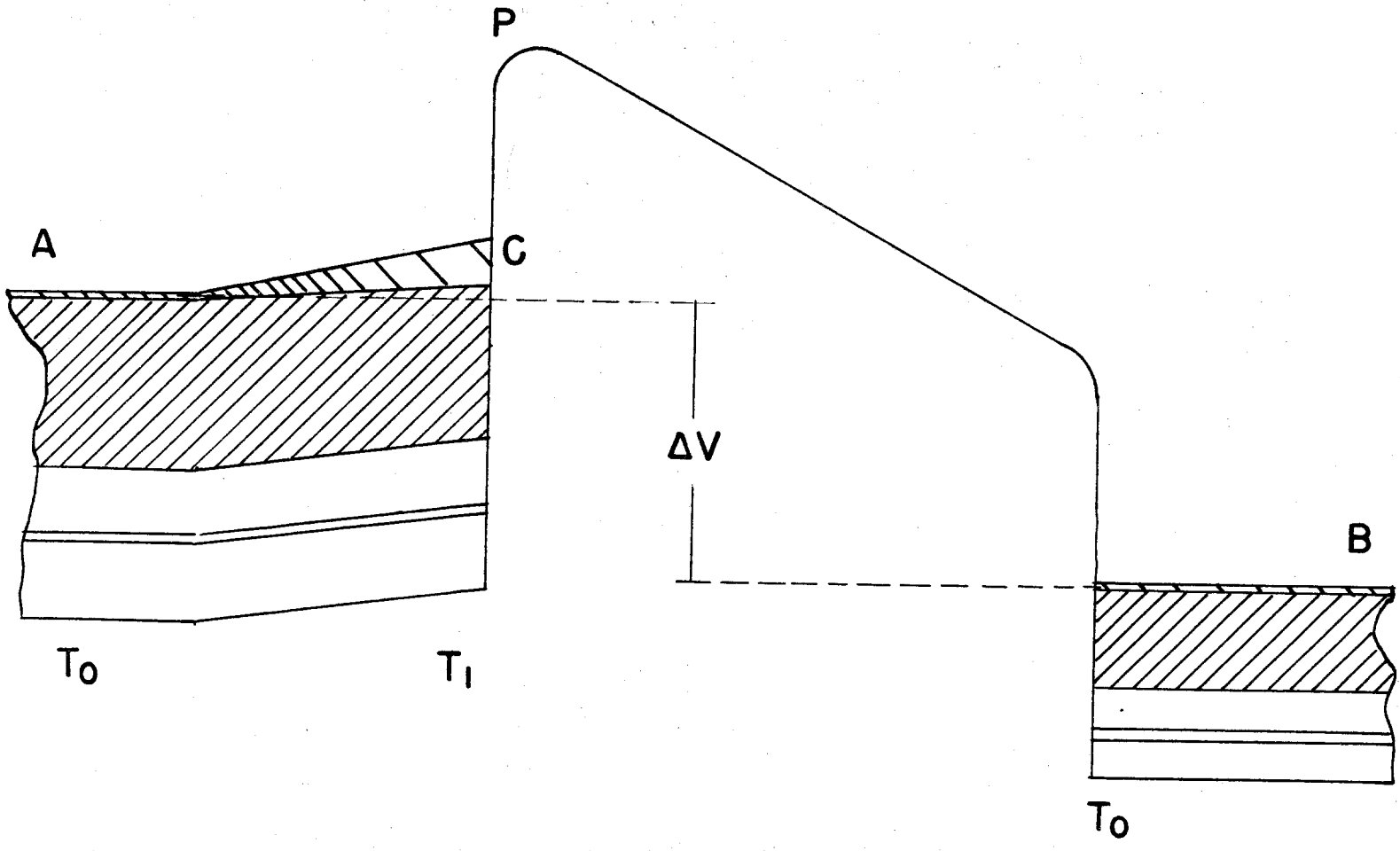

Fig. III

The voltage measured by the voltmeter corresponds to the difference in the mean upper edge of the Fermi levels at A and B. Due to the fact that the cathode is at high temperature the Fermi levels near the surface of the cathode (at C) will be widened near the edge. Simultaneously, however, the mean edge of the Fermi levels at C will be raised. This is accounted for by the fact that a temperature gradient exists from A to C and that here a few electrons will be transferred from C to A, raising the potential of C with respect to A until the retarding field caused by this potential rise will just equalize the forward and backward diffusion rates between A and C. This potential change corresponds to the ordinary Kelvin effect. It is, however, impossible to evaluate the energy shift from A to C by means of the ordinary Kelvin coefficient since from thermocouple measurements only differences of energy changes like these from A to C are known.

The energy given to an electron passing from C to P corresponds to the difference between the top of the surface potential energy barrier at P and the mean edge of the Fermi band at C, which is equal to the thermionic workfunction in the T^2 Richardson equation. This is strictly true only if 1) we can neglect the lowering of the workfunction due to the external field; i.e. we can use the zero field workfunction 2) we can neglect the thermal energy of the electron on leaving the cathode surface. The latter restriction can be removed if we add the mean kinetic energy corresponding to its electron temperature to the energy of the electron.

The energy of the electron available for conversion into

a quantum is therefore equal to

$e\Delta V$ + Single metal Kelvin P.D. from A to C + thermionic workfunction - Schottky's expression for the lowering of the workfunction due to an external field + mean energy of a free electron at its electron temperature.

For work at voltages $\Delta V = 20$ kV all terms but the thermionic workfunction term will be shown to be neglibable. We can, however, obtain a direct estimate of the total correction term (excepting for the field emission lowering of workfunction) by using data derived from calorimetric workfunction determinations. A calorimetric measurement of workfunction is made by measuring the extra power input required to maintain an emitter at constant temperature if an emission current is drawn from it. The workfunction thus measured will give the total correction required, provided that the extra power is measured across the cold ends of the filament leads rather than across the hot portion of the filament.

There is a considerable number of calorimetric determinations of thermionic workfunction in the literature.[73 - 84] The most accurate one of these is the one of Davisson and Germer[82 - 83]; unfortunately for our purposes the power input to the filament in their experiments was measured by attaching thin voltage leads to a hot portion of the filament; hence the Kelvin correction is not included in this work. The other experiments quoted are not as reliable in particular due to the poor vacuum conditions, never-the-less the result of

all these investigations gives results from .2 - .4 Volts. from the thermionic workfunction. The magnitude of the Schottky field correction can be estimated directly from the relation

$$\Delta b_o = 4.39 \sqrt{\frac{\partial V}{\partial x}} \qquad (2)$$

where b_o is the workfunction in degrees.(85) For $\frac{\partial V}{\partial x} \pm 10^4$ Volts /cm this gives $\frac{\Delta b_o}{b_o} \pm 10^{-2}$ for Tantalum; this is a negligable correction. From all this evidence it follows that for work at voltages of the order of 10^4 Volts or higher the only correction to be applied from this source is the ordinary thermionic workfunction, provided that an accuracy of less than 1 Volt is not aimed at.

A direct experimental proof of the necessity of the workfunction correction is furnished by the early work of Cooke and Richardson(75 - 76); in their work the power input into the anode of a diode is measured as a function of anode voltage; if the power is extrapolated to zero applied anode voltage the power expended is approximately equal to the product of the thermionic workfunction and the anode current. Despite the approximate nature of these early experiments they nevertheless demonstrate conclusively the necessity for such a correction to be made at all. In particular for the low voltage work of Oblin(26 - 28) this correction becomes of considerable importance (~.1% of the total voltage). The results of Oblin therefore must be corrected as shown, before correlating his results with those of other observers.

3) Analysis of a non-ideal isochromat

In addition to the workfunction correction other factors

prevent a direct application of the ideal eq. (1). Three of these factors, namely

1) Lack of monochromatism

2) Voltage drop along the filament

3) Ripple voltage

tend to render the intercept of the isochromat with the voltage axis asymptotic. Let us now consider the effect of a general "smearing" function on such an isochromat, without at first discussing the physical phenomena responsible for the existence of such a function.

The effect of voltage fluctuations, filament drop and ripple is to make the actual isochromat be a superposition of ideal isochromats with their voltage coordinates shifted.

The effect of lack of monochromatism is to make the actual isochromat a superposition of ideal isochromats taken at different wavelengths. If the wavelength at which a given isochromat is observed is shifted by an amount $\Delta\lambda$, then the Voltage intercept is shifted by an amount $\Delta V = -\frac{h}{e}\frac{\Delta\lambda}{\lambda^2}$; unless $\frac{\Delta\lambda}{\lambda}$ is very large the shape of the isochromat will be very little changed. A small shift in wavelength is therefore equivalent to a small shift in voltage of the amount given above. We can therefore treat the entire problem of the imperfect isochromat by assuming it to be composed of a set of perfect isochromats, the voltage axes of which are slightly shifted.

Let $y = f(z)$ be the equation of an ideal isochromat. The variable z is thus the independent variable i.e. z is proportional to the voltage coordinate. Let $F(z)$ be the experimentally observed function.

The variable y therefore, is proportional to the X-ray intensity. The operation of transforming f (z) into F (z) can in general terms be described as follows: $F_{(z)}$ is formed by a weighted superposition of the values $f_{(z)}$, evaluated at points neighboring to z. Let this weighting function be given by g (x) where x represents the difference in the coordinate of the f function to be weighted and in the coordinate of the point where F is to be evaluated. $F_{(z)}$ is then given by

$$F(z) = \int_{-\infty}^{+\infty} g(x)\ f(z-x)\ dx \qquad (3)$$

It is convenient to choose $\int_{-\infty}^{+\infty} g(x)\,dx = 1$. In the ideal case only the values of f evaluated at the argument of F itself receives weight; in this case g (x) and δ (x) and $F(z) = f(z)$.

Formally eq. (3) can be solved directly provided g (x) and F (z) are known for all values of the variable: Let Φ (t) be the Laplace or Fourier transform of $F_{(z)}$; Γ (t) be the transform of g (x) and φ (t) the transform of f (z); then (3) reduces to

$$\Phi(t) = \Gamma(t)\ \varphi(t) \qquad (4)$$

Hence the solution of (3) is a case of performing a Fourier or Laplace inversion. Practically this procedure is not feasable, however, principally because of the fact that neither g (x) nor F (z) are known well enough for values of the variables far removed from zero; in performing a reversion of this type the asymptotic behavior of all functions involved is of the greatest importance. Hence though the problem is a formally soluble one we are forced to adopt approximate methods adapted to our special conditions.

We can reduce eq. (3) to some extent by making use of the special properties of an ideal isochromat. Let us choose $z = 0$ to be the position of the shortwavelength limit of the ideal isochromat. Then

$$f(z) = 0 \qquad z \leq 0$$

$$F(z) = \int_{x=-\infty}^{x=z} g(x)\ f(z-x)\,dx \tag{5}$$

Again a solution of this eq. is formally possible and also the conversion of the integral into a sum provides a solutition by means of simultaneous equations; either method (being essentially the same) suffers from the difficulty of requiring a knowledge of the form of the "known" functions for large values of the argument.

For the purpose of locating the threshhold of the continuous spectrum it is not necessary to be able to solve eq. (5) for the function $f(z)$ for all values of z; the position of the intercept of the ideal isochromat is all that is of interest. Note that we cannot expect any abrupt changes in the actually observed isochromat; we rather have to devise a method by which we can infer as to the intercept of the ideal isochromat from the continuous variation of the real isochromat. Two such methods are available:

1) assume a convenient analytical form of $f(z)$ and $g(x)$ and compare the resultant expression of $F(z)$ (or at least some feature of it) to the actual isochromat.

2) examine certain properties of eq. (5) which can be considered without restricting the form of the functions involved excessively.

Method 1 has been used by Bailey[29] and DuMond[86]. They use

$$g(x) = \frac{1}{\pi a} \quad \frac{1}{(1 + \frac{x^2}{a^2})} \tag{6}$$

for the "smearing" function (in agreement with the theoretical and practical asymptotic behavior of crystal diffraction patterns) and

$$\begin{aligned} f(x) &= b\,x && 0 < x < Na \\ &= 0 && -\infty < x < 0 \\ &= 0 && Na < x < +\infty \end{aligned} \tag{7}$$

This gives

$$F(z) = \frac{bz}{\pi} \left[\tan^{-1}\left(\frac{z}{a}\right) + \frac{\pi}{2} - \frac{ab}{2\pi} \log \left\{ \frac{1 + z^2/a^2}{N^2 + 1} \right\} \right] \tag{8}$$

This expression is plotted in Fig. IV, together with the function $f(z)$. This figure shows that, provided the above assumptions are valid, the true intercept is given by the point of maximum curvature of the observed isochromat. It also shows that an extrapolation of the "linear" portions of the curves will lead to erroneous result; in fact the choice of the point whence the tangent is projected can give any arbitrary value to the measured limit.

Let us now examine certain properties of eq. (5). Differentiating twice:

$$F'(z) = g(z)\, f(0) + \int_{-\infty}^{z} g(x)\, f'(z - x)\, dx$$

$$= \int_{-\infty}^{z} g(x)\, f'(z - x)\, dx \tag{9}$$

since $f(0) = 0$

$$F''(z) = g(z)\, f'(0) + \int_{-\infty}^{z} g(x)\, f''(z - x)\, dx \tag{10}$$

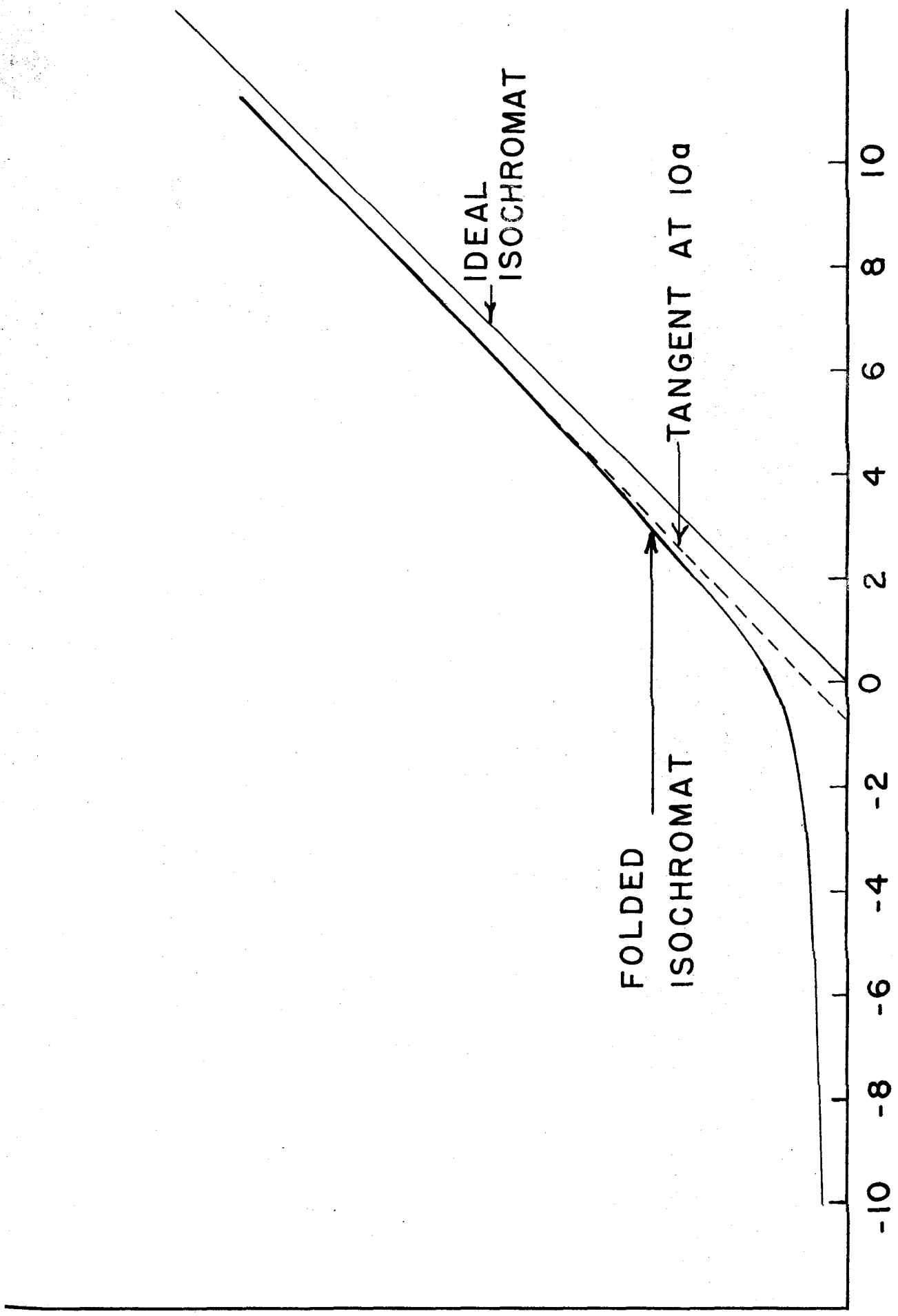
IDEAL
ISOCHROMAT
TANGENT AT 10a
FOLDED
ISOCHROMAT
10
8
6
4
2
0
-2
-4
-6
-8
-10

Fig. IV

Integrating by parts:

$$F''(z) = g(z)\, f'(0) - g(x)\, f'(z-x)\Big|_{x=-\infty}^{x=z} + \int_{-\infty}^{z} g'(x)\, f'(z-x)\, dx \qquad (11)$$

$$= \int_{0}^{\infty} g'(z-u)\, f'(u)\, du \qquad (12)$$

where $u = z-x$

Now let us assume that the "real" isochromat can be braken up into a set of straight line segments; i.e. let

$$\begin{aligned} f'(x) &= a_1 && 0 < x < x_1 \\ f'(x) &= a_2 && x_1 < x < x_2 \\ &\vdots \\ f'(x) &= a_i && x_{i-1} < x < x_i \end{aligned} \qquad (13)$$

then

$$F''(z) = \sum_{i=1}^{\infty} a_i \left[g(z - x_{i-1}) - g(z - x_i) \right] \qquad (14)$$

rearranging:

$$F''(z) = g(z)\, a_1 + \sum_{i=1}^{\infty} g(z - x_i)\, (a_{i+1} - a_i) \qquad (15)$$

This is the finite difference equivalent of eq. (10) in the form

$$F''(z) = g(z)\, f'(0) + \int_{0}^{\infty} g(z-u)\, f''(u)\, du \qquad (16)$$

Eq. 15 is the equivalent of the geometrical analysis of DuMond and Bollman[25]. It shows that the second derivative of the observed isochromat is proportional to the "smearing curve" $g(x)$ excepting for a correction term

$$\sum_{i=1}^{\infty} g(z - x_i)\, (a_{i+1} - a_i) \qquad (17)$$

This term represents the influence of any changes in slope on the curvature at the origin; unless a large change in slope occurs only a small distance away, as compared to the width of the "smearing" function $g(x)$, from the point $z = 0$, this term will be both small in magnitude and slowly varying. Hence

$f''(z) = g(z)a_1$ will reach a maximum which we assumed to be at zero; hence the intercept of the "true" isochromat, to a very good approximation, coincides with the point of maximum 2nd derivative of the observed isochromat. In discussing our actual results we will actually estimate the size of the correction given by eq. (17). The form and width of the smearing function will be discussed in connection with the analysis of the experimental results.

III Experimental Arrangements

The essential components constituting the apparatus for the type of h/e determination described here are

1) H.T. D.C. Powersupply and controls

2) Filament powersupply and controls

3) X-ray tube

4) Voltage measuring devices

5) Monochromator

6)Ionchamber and associated instruments

The precision attainable in this experiment is essentially limited by two factors: first, the available intensity in the neighbourhood of the shortwavelength limit as compared to the sensitivity and stability of the detecting device and secondly the precision to which the high tension d.c. Voltage applied to the X-ray tube can be controlled and measured.

The intensity near the limit is essentially determined by three principal factors: First, the primary energy in the electron beam; secondly the anode material, and third the geometry of the monochromator arrangements. Since the latter is generally determined by other factors, the available intensity is principally a function of the X-ray tube power. The use of the thirty kilowatt X-ray equipment constructed by DuMond and Youtz[87] constitutes therefore an essential step in improving the attainable precision of this experiment.

1) The D.C. Powersupply

A schematic diagram of the D.C. Powersupply aso originally designed is shown in Fig. V. The primary of a high voltage

45 kVA power transformer is fed by an 150 cycle alternator driven by a synchronous motor. The field of the alternator is separately excited by a generator on the same shaft. The power input to the transformer is controlled by a set of 3 rheostats in series with the alternator field (Fig. 10 ref. 29). V_1 and V_2 are high-vacuum continuously pumped high voltage Kenetrons; they contain a V-shaped 80 mil tantalum filament operating at 13V RMS, 110 Amperes from insulation transformers; at this filament power the saturation current is about 1 Ampere. The plates of the Kenetrons are watercooled with water supplied through 100 feet of coiled thick-walled rubber hose. The watercooled anode and the filament are assembled in a transformer type porcelain bushing. The condensers shown are composed of 3 1/4 μF 50 kV Cornell Dubilier condensers in series. The chokes have an inductance of 1000 Henry at 100 ma d.c. load; they are oil immersed and are wound on a nearly closed core with 2.5 millimeters air gap. The resistances shown in the diagram are sections of water carrying rubber hose. Further details regarding the circuit components are given in the original article[87] describing this equipment.

Since all of the work described here and a good part of the work contemplated in the near future requires a voltage less than 50 kV, it was decided to convert the voltage doubling circuit of Fig. V temporarily into a single ended half wave rectifier (Fig. VI). The two Π filter sections were connected in series; the condenser constituting the original 1/12μF condenser groups were converted into .75μF units by parallel connection. This does not apply to the input condenser; it was maintained at 1/12μF in order to avoid excessive peak

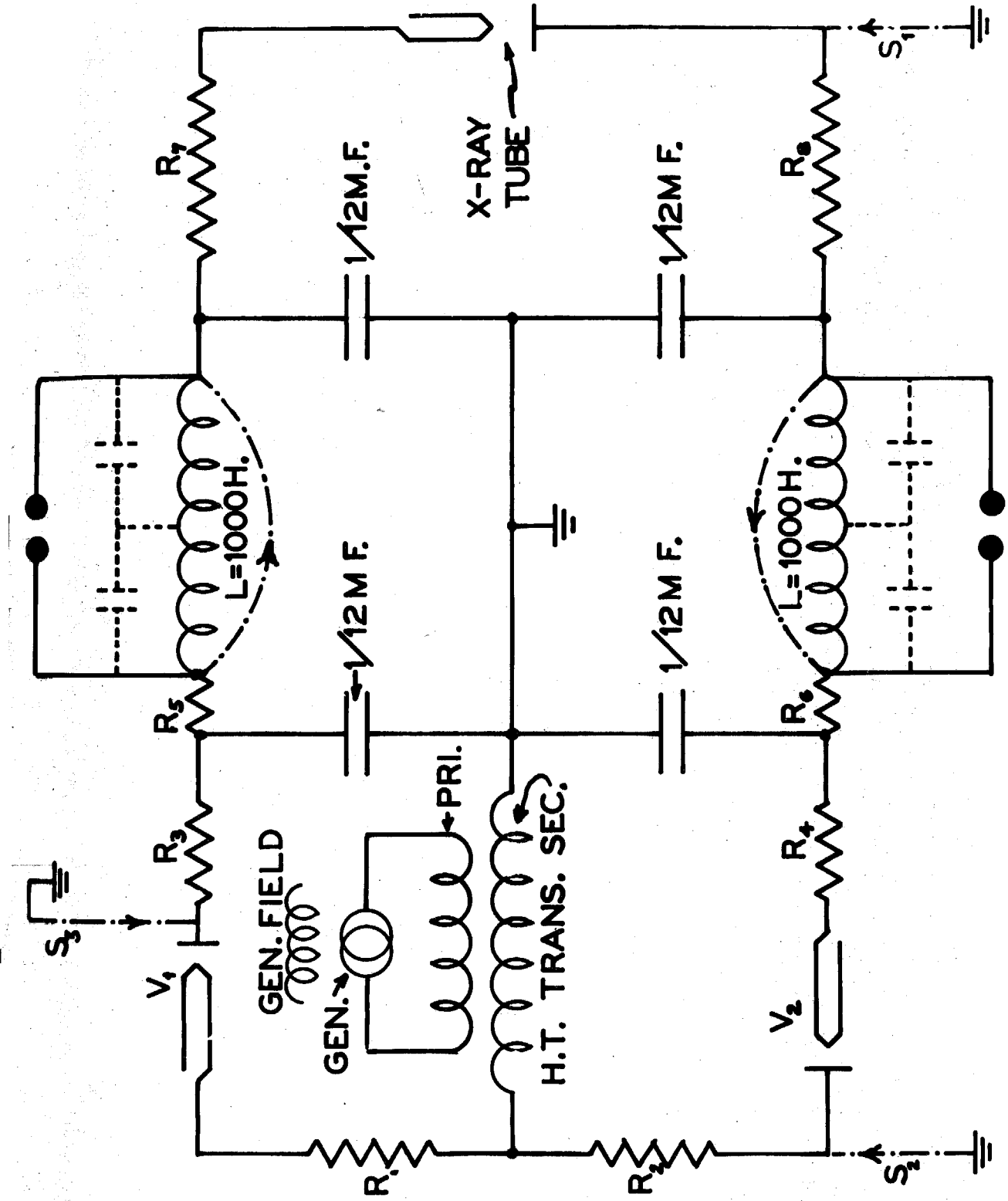
R7
1/2M.F.
X-RAY TUBE
1/2M.F.
R8
S1
L=1000H.
L=1000H.
R5
1/2 M F.
1/2 M F.
R6
R3
PRI.
H.T. TRANS. SEC.
R4
S3
V1
GEN. FIELD
GEN.
V2
R1
R2
S2

Fig. V

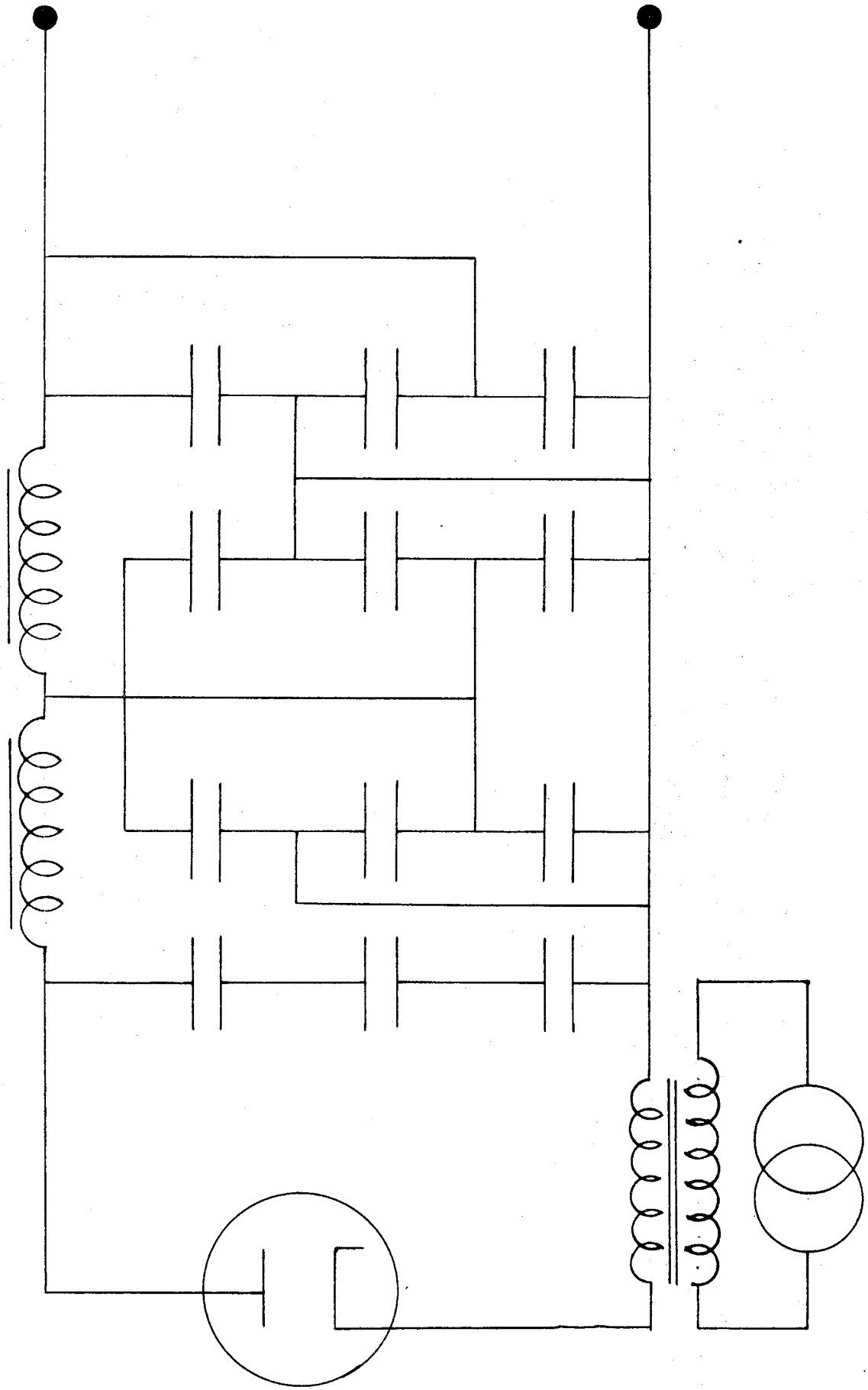

Fig. VI

currents through the Kenetron. The peak current through the Kenetron was measured by observing oscillographically the drop across a 1 Ω resistor in series with the ground end of the input filter condenser; it was found to be 500 ma at a 100 ma load.

2) The Voltage Regulator.

Despite the care taken in making the input power independent of line voltage fluctuation, fluctuations of several hundred volts are observed in the output voltage of this power supply. These fluctuations are principally caused, we believe, by fluctuations in the filament emission of the X-ray tube caused by filament voltage fluctuation combined with emission changes caused by changing vacuum conditions. Because of the large regulation of the powersupply these changes in emission can easily account for the observed fluctuations. In addition to this source of fluctuation, part of the observed voltage changes may be due to changes in alternator brush resistance; uncertain contacts in the power transformer primary circuit; irregular leakage current along the rubber hoses carrying cooling water; variations in power frequency. Special care was taken to reduce brush and contact errors to a minimum.

In order to reduce the voltage fluctuation discussed above an automatic voltage regulator was introduced into the power supply circuit. The regulator is of the vacuum tube, degenerative type[88]. Its position in the powersupply circuit is shown in Fig. VII and its detailed circuit diagram in Fig. VII. Qualitatively its operation is as follows: The voltage divider, $R_1 - R_o$ divides the voltage across the X-ray tube in the ratio

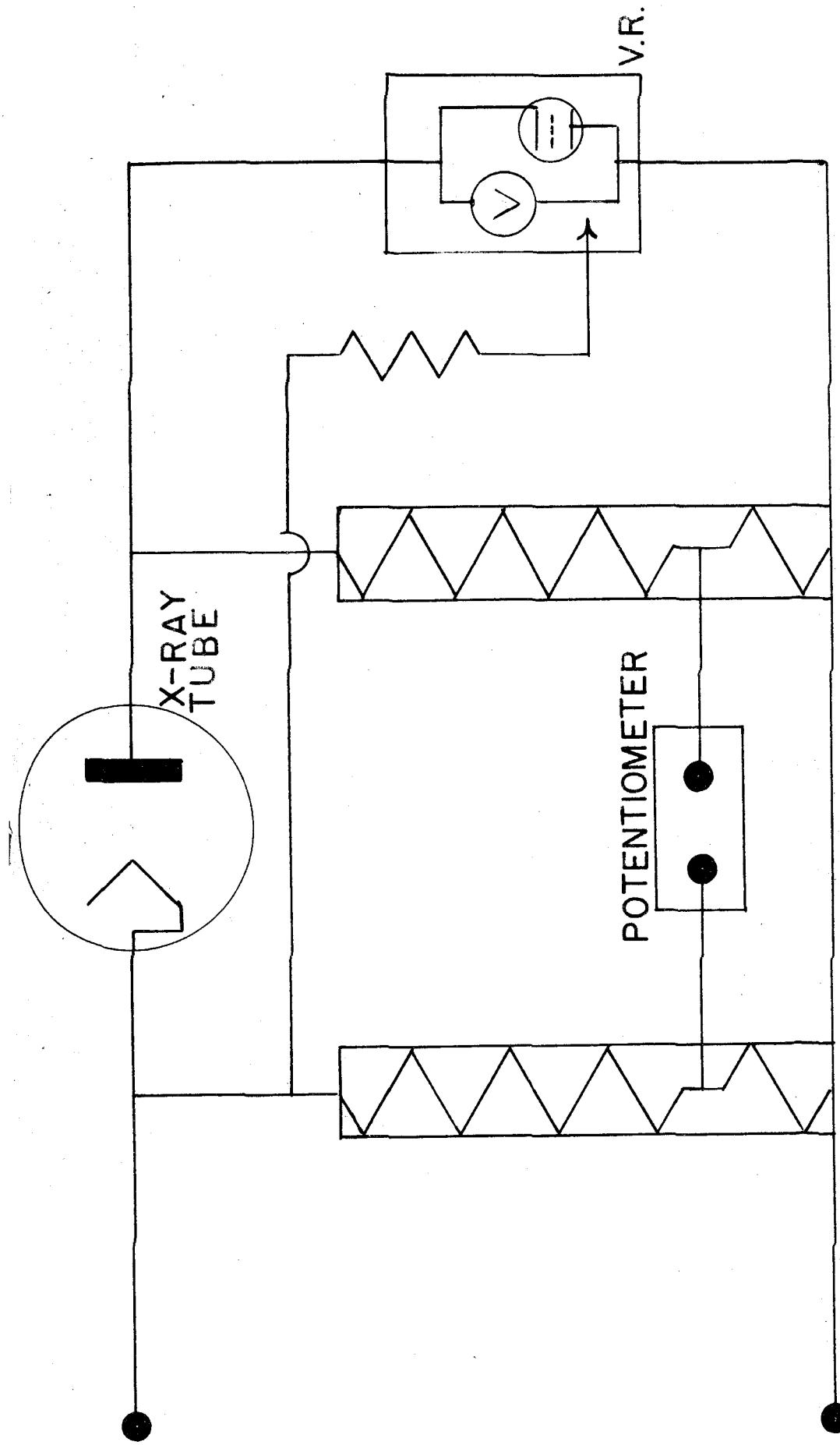

Fig. VII

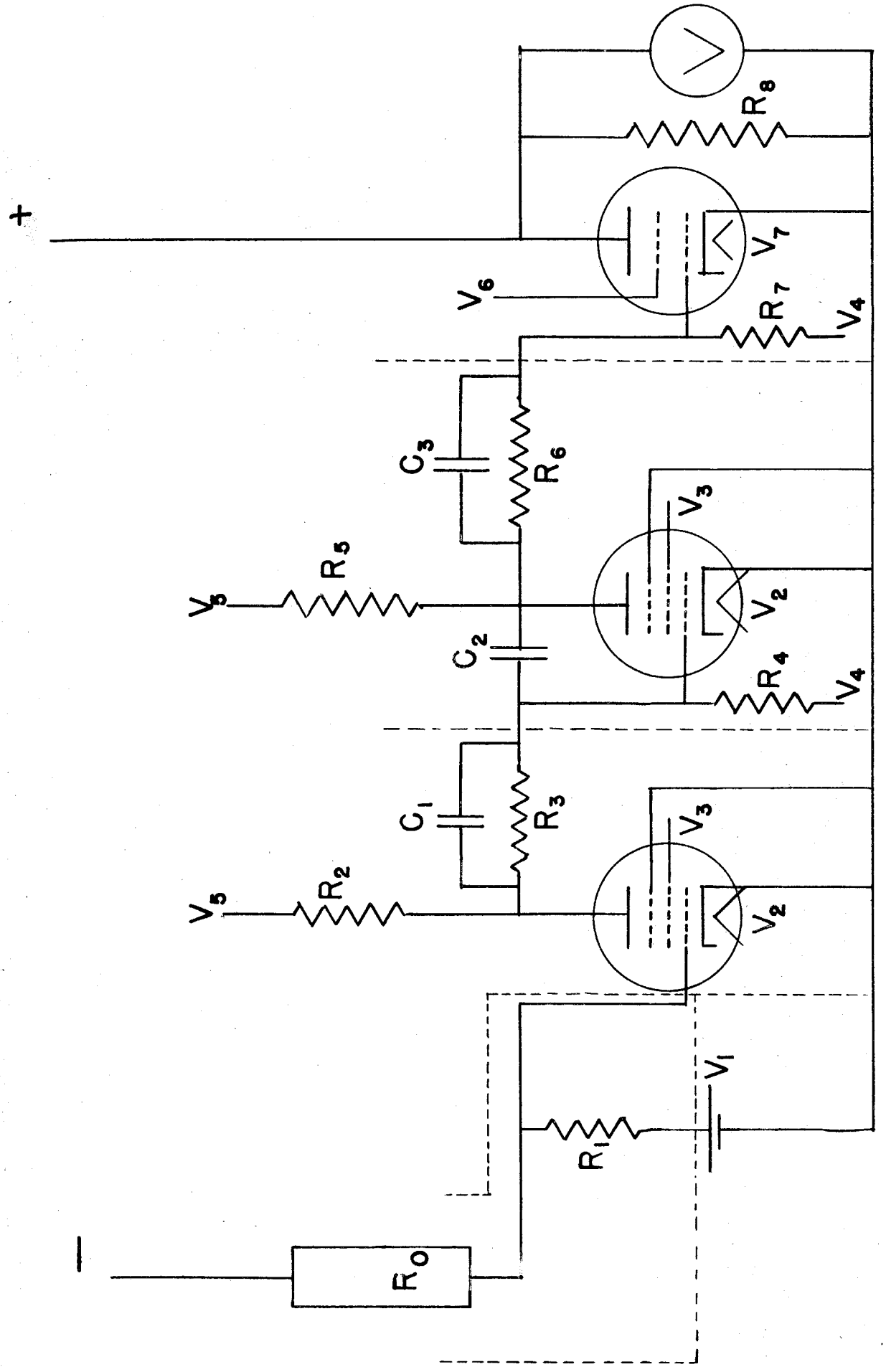

Fig. VIII

1:400; any changes in this voltage are amplified by a 3 stage d.c. coupled voltage amplifier and, through the power stage, are applied in series with the line from the powersupply to the X-ray tube. The phase is such that the action is degenerative. The bias on the first tube of the d.c. amplifier is supplied by an adjustable voltage provided by batteries. It is the value of the voltage of these batteries which determines at which value the high voltage will be stabilized. Let the overall voltage gain of the amplifier be Γ. Let us consider a fluctuation which ordinarily would cause a voltage change of ΔV_o Volts, and let the action of the regulator reduce this fluctuation to ΔV. It follows then that

$$\Gamma \frac{R_1}{R_o} \Delta V = \Delta V_o - \Delta V \qquad (18)$$

and hence $$\Delta V = \frac{\Delta V_o}{1 + \Gamma\left(\frac{R_1}{R_o}\right)} \sim \frac{\Delta V_o}{\Gamma \frac{R_1}{R_2}} \qquad (19)$$

if $\Gamma \frac{R_1}{R_o} >> 1$.

For our circuit parameters the gain of each of the first two stages can be shown to be 100 approximately; the gain of the power stage is about 20, making $\Gamma = 200{,}000$. The feedback ratio $\Gamma \frac{R_1}{R_o}$ is therefore 500 approximately, showing that any fluctuation will be reduced in the ratio 1:500. The gain of the circuit was tested by direct measurement. The Resistance R_8 in parallel reduces the amplification of the last stage; its function is to limit the drop across the power absorbing stage to 750 Volts when a current of 100 ma is flowing, thus making any safety devices for limiting the voltage drop unnecessary. The instrument is protected against surges by the

standard fuse-cigarette-paper high voltage safety device.

Because of the fact that the power absorbing capacity of the regulator is small, manual control is required in addition to the automatic stabilizer; the operator controls the primary voltage so that the Voltmeter V across the power tubes stays within a range of say 250 Volts; the high voltage then stays constant to 1/2 Volt. The value of the stabilized high voltage depends on the setting of the variable battery V_1. The procedure for setting at a given value of the X-ray tube voltage is as follows: The potentiometer measuring the high voltage is set at the required value; balance on the potentiometer galvanameter is then obtained by adjusting the battery V_1 while a second operator controls the primary voltage such that the voltage drop across the regulator does not vary outside its permissable range. The voltage adjustment is thus made simply by adjustment of V_1. Since the power to supply V_1 is derived from batteries which are likely to drift in voltage, slight readjustments of V_1 are occasionally necessary in order to keep the potentiometer balanced. With these operations it is possible to keep the voltage constant to 1/50,000 for long periods of time with occasional interruptions due to the operator not following the voltmeter rapidly enough.

One of the principal difficulties encountered with a regulator of this kind is the problem of oscillations. If one looks at the regulator circuit as an amplifier with very strong inverse feedback (feedback ratio of 500) than it is evident that if there is a frequency at which the phase shift throughout the whole amplifier becomes 180° and at which the

gain has not dropped by more than a factor of 500 as compared to the d.c. amplification, then oscillation will occur. If one draws the equivalent circuit of the d.c. amplifier of Fig. VIII, it will appear to consist of 6 L sections of the type shown in Fig. IX.

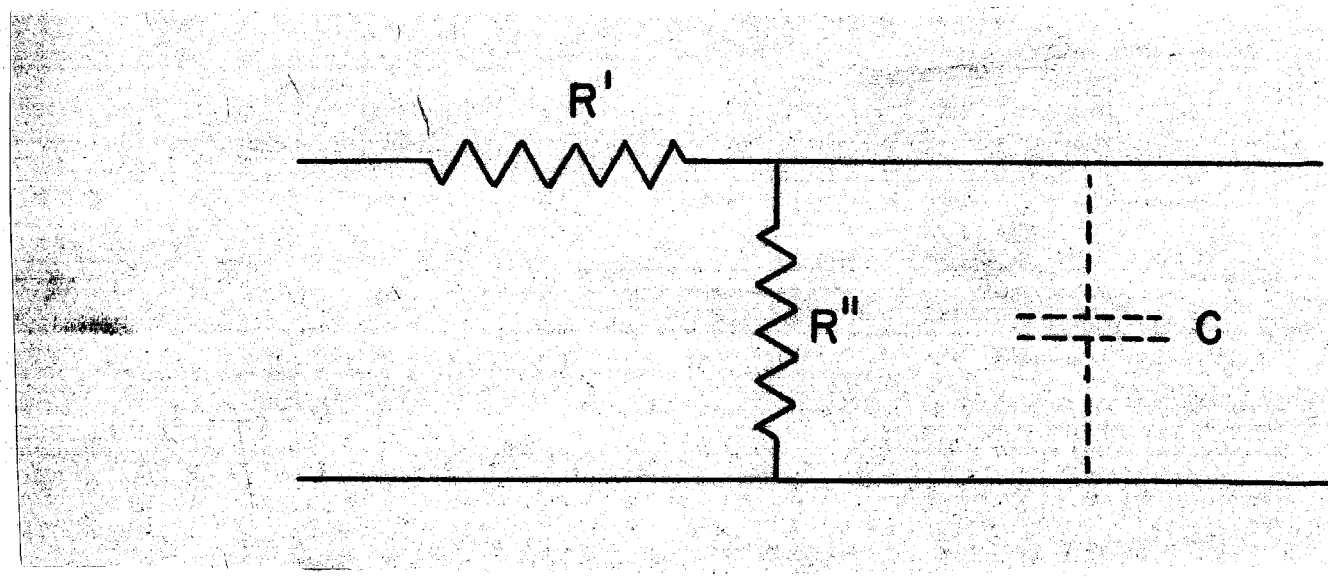

C here represents the distributed capacity to ground. Each of these sections can give rise to a phase shift φ at most equal to 90°; the overall amplification is then decreased by a factor cos φ for each section. Hence, if the shift is 30° per section, the overall phase shift is 180° but the gain is decreased by $\left(\frac{\sqrt{3}}{2}\right)^6 = .42$ only, and hence oscillations will occur. The only way, therefore, to prevent this system from oscillating is to make the frequency response of the different stages very unequal. If this is done the gain of one stage will have fallen by a large amount before the other stages cause appreciable phaseshift. A suitable way of achieving this purpose is to introduce the condensers C_1, C_2, and C_3 as shown in Fig. VI . C_1 and C_3 simply unite two pairs of the L sections of the equivalent circuit into two single sec-

sections, thus increasing the necessary phaseshift per section necessary for oscillation. C_2 modifies the frequency response of the second stage by introducing inverse feedback at high frequencies. This method of introducing a decrease of amplification at high frequencies has a considerable advantage over an ordinary shunt condenser to ground: it introduces no phase shift at high frequencies. This can be shown as follows:

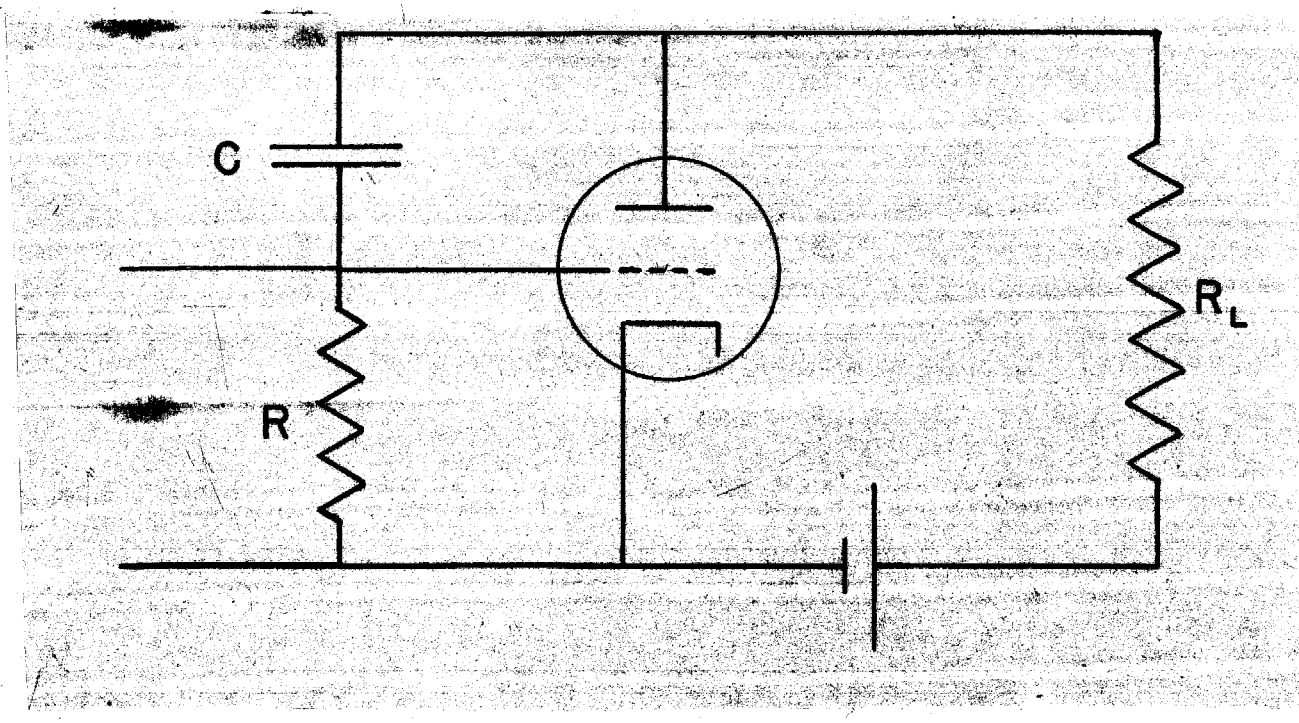

Let e_{go} be the externally applied signal. The circuit equations are:

$$e_g = e_{go} + \frac{R}{R - \frac{1}{\omega C}} \qquad (20)$$

$$e_p = -\mu e_g \frac{R_L}{R_p + R_L} \qquad (21)$$

If we let $G_o = \frac{\mu R_L}{R_p + R_L}$ stand for the gain of the stage without feedback, then the solution of the circuit equation is

$$G = \frac{G_o}{1 + G_o \dfrac{R}{R - \dfrac{1}{\omega C}}} \qquad (22)$$

where $G = \dfrac{e}{e_{g_o}}$ is the actual gain of the circuit.

The phaseshift ψ is given by

$$\psi = \tan^{-1} \left\{ \frac{G_o \sin 2\varphi}{2 + G_o + G_o \cos 2\varphi} \right\} \qquad (23)$$

where $\tan \varphi = \dfrac{1}{R\omega C}$ (24)

Hence the gain G is equal to G_o at low frequencies but falls to

$$\frac{G_o}{1 + G_o} \sim 1$$

at high frequencies. The phaseshift is zero both for very high and very low values of the frequency; it raises to a maximum value .

$$\tan^{-1} \left\{ \frac{G_o}{2 + G_o} \right\} \sim \frac{\pi}{4}$$

at the frequency given by $R\omega C = 1$. It is seen, therefore, that this circuit causes a decrease in gain by a factor of $\dfrac{1}{G_o}$, this decrease becoming effective at a frequency greater than $\omega = \dfrac{1}{RC}$; this decrease in gain will not cause any appreciable phase shift at high frequencies. The advantage of this system of making the gain of the various stages unequal was verified by the fact that a condenser of only $C_2 = 1000\ \mu\mu F$ sufficed to suppress all oscillations. Unfortunately it was necessary to make $C_2 = .25\ \mu F$, since even though the phase shift at ripple

frequency (15 0~) was not sufficient to cause re-generation, nevertheless because of the fact that the input and output of the regulator did not exactly cancel one another the ripple was actually increased by the regulator action. The increase of C_2 to .25 μF suppressed this effect.

The regulator and the supply batteries are housed in an iron framework clad with galvanized iron; the entire assembly is insulated from ground through a micarta column. All stages are carefully insulated by shielding. Power is supplied to the 6 L 6 heaters and the screen powersupply through an insulation transformer. All other power is derived from batteries.

3) The Filament Supply.

Because of the large regulation of the set (caused principally by the small size of the input condenser and the leakage reactance of the power transformer) stability in emission current, and therefore stability in X-ray filament power is of greatest importance if voltage stability is essential. If the tube is operating saturated, then the essential part of the Richardson equation is $i = Ae^{-\frac{\varphi}{T}}$; and hence $\frac{\Delta I}{I} = \frac{\varphi}{T}\frac{\Delta T}{T}$; from the Stefan-Boltzman relation $\frac{\Delta T}{T} = \frac{1}{4}\frac{\Delta W}{W}$ where W is the filament power; hence

$$\frac{\Delta I}{I} = \frac{\varphi}{4T}\frac{\Delta W}{W} \qquad (25)$$

If we put $\varphi = 50{,}000$ $T = 200$, this gives

$$\frac{\Delta I}{I} = 6\ \frac{\Delta W}{W} \qquad (26)$$

approximately. The regulation of the set is such that, near the point where most of our data were taken, a change of 5 ma

emission current causes a change of 2 KV in the operating voltage. Hence if I = 100 ma, V = 20 V

$$\frac{\Delta V}{V} = \frac{2000}{.005} \cdot \frac{.1}{2 \times 10^4} \frac{\Delta I}{I} = 2 \frac{\Delta I}{I}$$

Hence

$$\frac{\Delta V}{V} = 12 \frac{\Delta W}{W} \qquad (27)$$

i.e. the filament power has to be 12 times more stable than the required voltage stability.

In order to assure filament power stability the filament was supplied by three 21 KL Globe Union 1000 Amp rating glass jar storage batteries. These batteries were continuously charged by two 300 watt d.c. airplane generators driven by an insulating belt from a 1 h.p. motor at ground potential. In the majority of the cases when trouble due to fluctuations was encountered, the cause was traceable to variations in the charging rate of the generators. If the generator voltage changes by an amount ΔV_o, the voltage change across the filament is given by $\Delta V' = \Delta V_o \frac{r}{R}$ approximately, where r is the interval resistance of the batteries and R the resistance of the generator circuit. In order to reduce $\Delta V'$ for a given ΔV_o, R was artificially increased by inserting a resistor of about .1 Ω, made of 8 #14 manganin coils soldered into copper bus bars, into the generator circuit. The charging rate is controlled by Centralab 25 Watt Radio rheostat inserted in series with the field coils of the generator. The filament current (about 30 Amp) proper is controlled by a monel tubing rheostat of total resistance variation of .1Ω; a .008" wall monel tube is placed in series with the filament. A flask, tubulated at the bottom, is connected through Koroseal tubing

to the bottom of the monel tube. If the flask is filled with mercury, a mercury column can be raised and lowered inside the monel tube, by simply raising and lowering the flask. It is thus possible to vary the resistance between the ends of the tube because a variable part of it is shortcircuited by the mercury. Details of construction of this rheostat as well as the details of mechanical assembly of the filament supply circuit are described by Bailey[29]. This method of filament control proved to be exceedingly satisfactory at first, - both from the point of view of stability and smoothness of control. After prolonged use, however, the resistance changes caused by the change in mercury level became discontinuous, probably due to impurities on the inside of the monel tube. The difficulty inherent in all mercury type rheostats constructed so far (see e.g. C. R. Barber[89]) caused by contamination of the electrodes has therefore not been solved as yet in the present design.

In order to assure stability of filament operation it was found to be particularly necessary to eliminate all sliding contacts, such as mechanical rheostats, knife-switches (replaced by copper links immersed in mercury pools) or relay contacts. The only point where mechanical contacts were unavoidable, namely on the commutators of the charging generators, was a frequent source of trouble. This trouble was partially allayed by careful turning and undercutting of the generator armatures. The size of all wiring was still further increased. The combination of all these precautions resulted in a filament supply stable enough for our purpose; it is believed, however,

that the voltage fluctuations still remaining across the X-ray tube are still principally caused by filament circuit instability.

4) Modifications in design of the X-ray tube

The X-ray tube used was the tube built by DuMond and Youtz[87] and constructional details can be found in their paper. In order to adapt this tube to our present purpose a number of changes were made which will be described here.

A point of considerable importance for a study of the shortwavelength limit of the continuous spectrum is the constitution of the target surface. The efficiency of the production of the continuous spectrum is proportional to the atomic number z of the target material; hence if the target is composed of layers of different materials, each layer being only a "few Volts thick"*, then the shape of the continuous spectrum near its shortwavelength limit will be profoundly altered. Such a layer structure of the target can be caused by two sources: 1) evaporation of filament material onto the target and 2) deposits on the target caused by the ion bombardment of the target. The first cause of a layer structure is in general not of great importance for the following reasons: in order to obtain high intensity in the continuous spectrum near its limit it is of course advantageous to use

* By the "thickness in volts" is meant the energy loss of the electron beam in traversing a given thickness measured in electron volts. The continuous spectrum as ordinarily observed from a thick target can be imagined as being the superposition of a set of thin target spectra produced by electrons of varying amounts of energy, depending on the depth of the layer under consideration. A thin target spectrum, if plotted on a frequency scale, is approximately a uniform rectangular distribution extending to the shortwavelength limit. A thick target spectrum in a pure metal will then show a nearly linear rise near the limit, since it is formed by superposition of such rectangles with their shortwavelength limit continuously receding towards higher wavelength.

a high atomic number target material; since X-ray tube filaments are generally made of Tungsten (z = 74) or Tantalum (z = 73), a deposit of such materials would not materially change the efficiency of production of the continuous spectrum. The effect of such deposits does, however, become important if studies of the continuous spectrum of low atomic number materials are contemplated. For instance, the isochromats of Schwarz and Bearden[30] taken with a copper and a nickel target are probably in reality tungsten curves as can be concluded from the fact that the slope of the isochromats near the limit is not materially different from that of the curves published for a gold target. In this work the target was made by amalgamation of a gold layer onto a copper target (by the process described by DuMond and Youtz[87]) and the filament is made of tantalum; also in our later curves the cathode was reconstructed such as to shield the filament; hence we are here not concerned with deposits from the filament.

The second source of deposits, namely the deposits due to ion bombardment is a much more serious one. The reason is that in a tube such as the one used here the deposit is most likely to contain carbon as its principal component. The reason for this is the fact that a considerable part of the residual gases in the tube are due to organic vapors from the gaskets or from the oil diffusion pumps. A layer of carbon on the target surface would slow down the electron beam accompanied by X-ray production of only 1/13 the intensity of that obtained from the gold target; hence since the intensity of the continuous spectrum is very close to the limit of observation at points near the shortwavelength limit, the X-rays from the carbon

would probably escape observation altogether. The effect of such carbon deposits would therefore be to cause an apparent shift in the position of the isochromat along the voltage axis; this shift would correspond to higher values of h/e.

An obvious cure would be to prevent the existence of such deposits by a thorough trapping of all condensible vapors. The charcoal trap originally intended for this purpose was found to be impractical. It was replaced first by a conventional design glass trap, but owing to the fact that this trap decreased the pumping speed by an excessive amount it was replaced by a trap of different design. The trap now in use consists of a cylindrical copper pot of 3" height and 3" in diameter suspended by a thin German silver tube. This trap will hold liquid air for about 9 hours. The pump was removed from its position directly under the X-ray tube; in its place a valve driven through a ball and socket joint and sylphon arrangement was installed (Fig. XI). The liquid air trap described above is placed between the valve and the pump. The pumps are of 3" and 6" diameter and are of the Hickman self-fractionating type. The details of the pump design are given by Bailey[29] and DuMond and Youtz[87]. In order to prevent excessive transfer of oil to the liquid air trap a set of baffles was installed in the upper end of the 6" pump. These baffles were originally intended for refrigeration but tap water circulation through the baffle proved to be equally effective.

These attempts in preventing carbon deposits retarded the rate of formation of these deposits appreciably but did not

succeed in their complete prevention. It was therefore decided to make use of the lower valve of the X-ray tube for purposes of mounting on it a device for cleaning the target without the necessity of breaking the vacuum. The design finally adopted is shown in Fig. XI. An arm A is mounted on an upright post B attached to the stationary plate C of the valve. This arm is driven through an adjustable rod D from the movable plate E of the valve. This rod has two balls silver-soldered in its ends; these balls are engaged by cups on the valve plate and the scratcher arm A respectively. The entire device is constructed so that all adjustments can be made through the rear windows of the X-ray tube. The moveable arm carries the "scratcher" proper. The target deposits turned out to be quite hard, so attempts to construct the "scratcher" of steelwool, spot welded to springsteel, were not successful. The scratcher which was finally used is shown in Fig. XII. It consists of a large number of pieces of piano wire each about 1/2" long soldered into a brass ring. In order to construct this brush the piano wire sections were pushed into the end-grain of a stick of balsa wood and the ring was placed around the ends sticking out and solder was poured into the inside of the ring. This method of assembly prevents the solder from diffusing out to the ends of the wire which should remain free. The ends of the wires were then ground to a suitable surface. The cleaning of the target is performed by closing the bottom valve on the X-ray tube and then turning the gyrating target drive. The device is adjusted such that the brush is directly opposite the center of the filament cup if the valve is closed; the gyration of the target will then cause the brush to move around

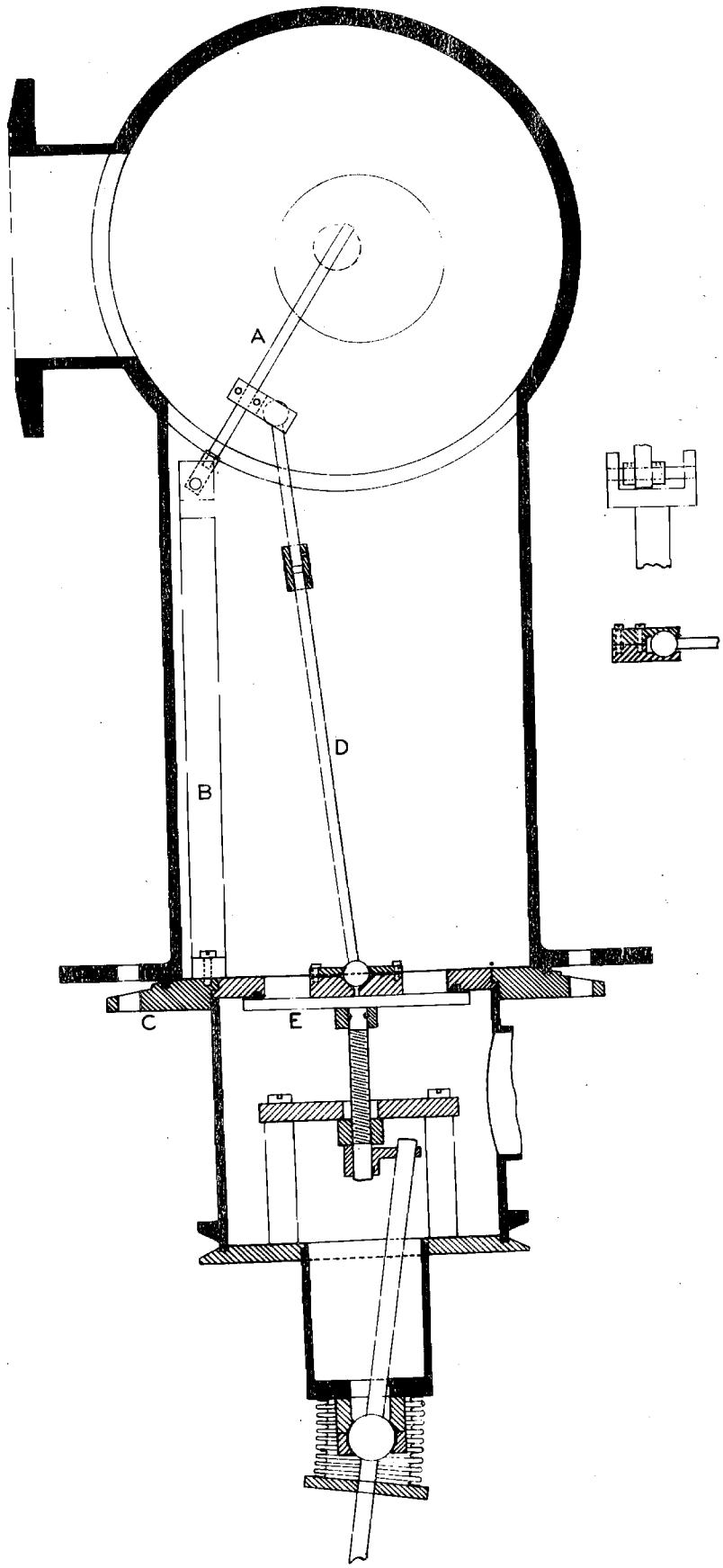

Fig. XI

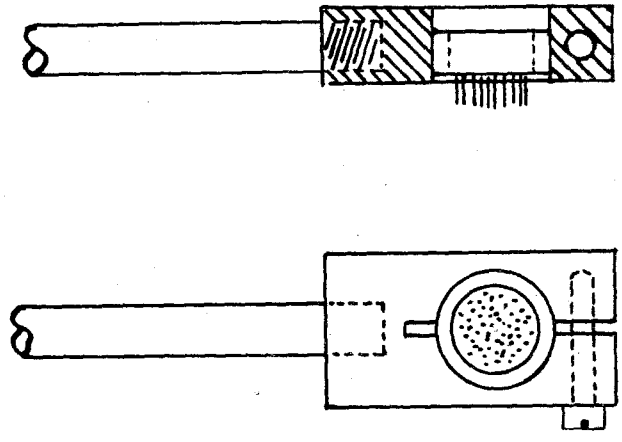

Fig. XII

the focal circle.

The effect of the internal cleaner on the measurements was quite evident. Fig. XIII shows two isochromats; the (A) curve is obtained after the tube had been in operation without cleaning the target for a long time; the other curve (B) is observed with the "scratcher" in operation between every two or three measurements. It is seen in this case that the cleaning process causes a shift of nearly 1% in the abscissae of each point, corresponding to an equal change in the value of h/e. The curves also show that the carbon radiation is not observable, at least not with the detection sensitivity used when those points were taken.

These results show that values of h/e obtained by the use of continuously pumped X-ray tubes must be considered unreliable unless precautions similar to the above are taken. The rate at which deposits are formed is of course smaller at smaller tube currents; also in commercial, sealed off, carefully de-gassed, glass tubes organic vapors are possibly not present. Hence the effect of carbon deposits demonstrated here has possibly no bearing on the results of former work on this subject, excepting on the work of Ohlin[26 - 28]. Ohlin uses an oil diffusion pump at his final pumping stage and employs rubber tape gaskets; the presence of organic vapors can therefore be inferred. Whether deposits of sufficient thickness to influence his results were formed in his case, is of course difficult to judge. Since Ohlin was working at voltages from 3000 - 5000 Volts, only a layer of 4 Volts "thickness" is required to cause an error of 1/10,000; this requires only a layer of 10^{-8} cm (!), using the expression

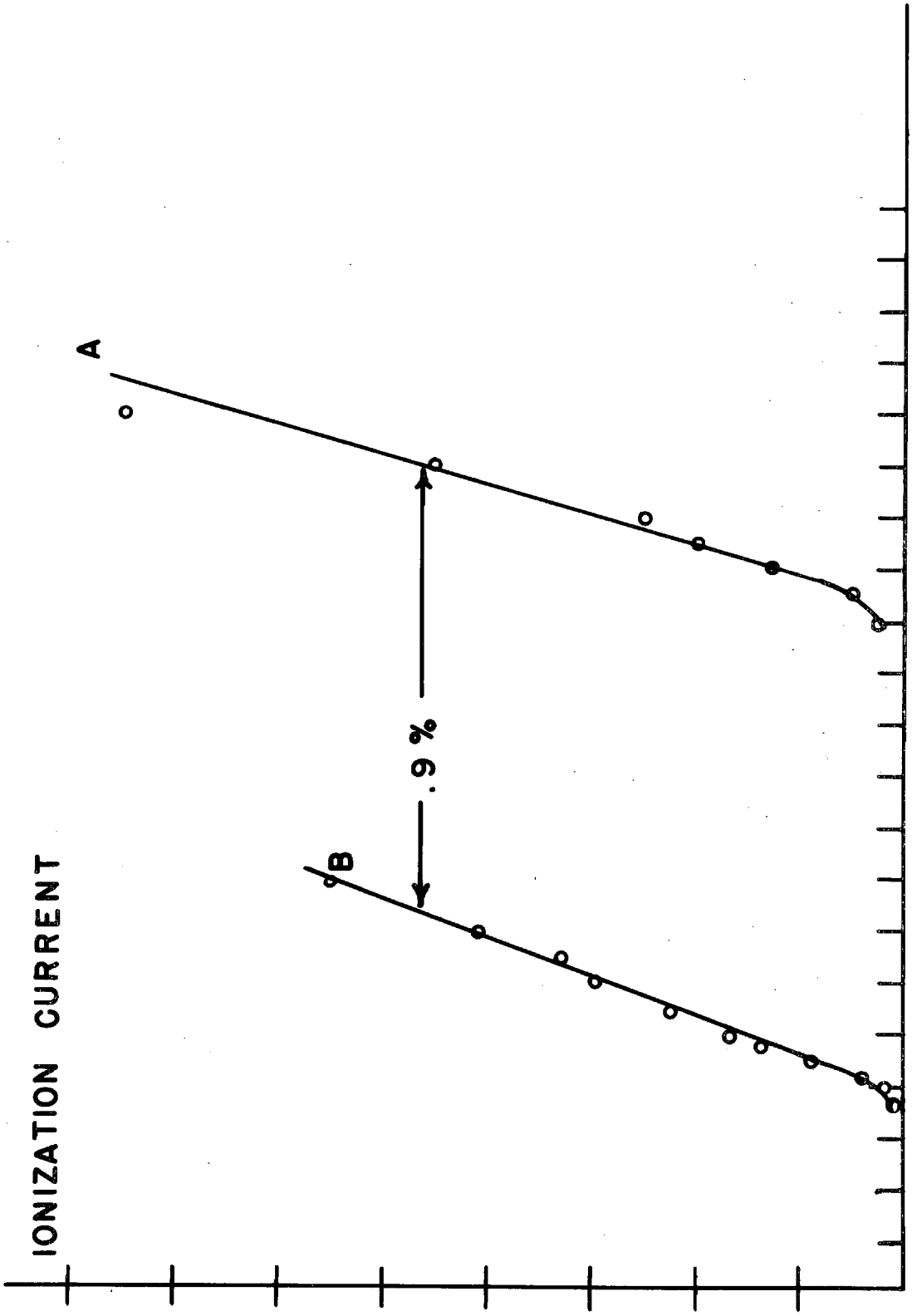
IONIZATION CURRENT
A
B
.9 %
10060
10100
10140
10180
POTENTIOMETER SETTING

Fig. XIII

for electron stopping power given by E. J. Williams[91]. Hence a deposit only a few molecular layers thick would seriously impair the accuracy of Ohlin's results. On the other hand a layer as much as 10^{-5} cm thick would require so much energy to penetrate that in that case simply a correct isochromat corresponding to a carbon target would be obtained.

Another important change made in the X-ray tube is the re-design of the cathode. The original filament was made of tantalum coiled in the form of a conical spiral; the filament was placed inside a shield cup. The hole in the front of the cup was of sufficient size such that the entire filament was in view of the target. It was thought advantageous to replace this type of cathode construction by an indirect cathode as had been done successfully by other investigators.[92 - 94] For this work the principal advantage of such a construction is the fact that the filament is not subject to positive ion bombardment; hence the emission remains steady even under not too good vacuum conditions. The design of the new filament mounting is shown in Fig. XIV (taken from Bailey[29]). The filament is in the form of two nearly complete circles held in place by tantalum hooks. The hole in the frontcover of the assembly is slightly smaller than the diameter of the circles. Any positive ion bombardment will impinge on parts electrically connected to the shield and not to the filament; it is thus possible to study the effect of any secondary electron.

Ohlin[27] describes an effect of the X-ray tube pressure both on the shape and position of the isochromats. He attributes this effect due to the presence of secondary electrons

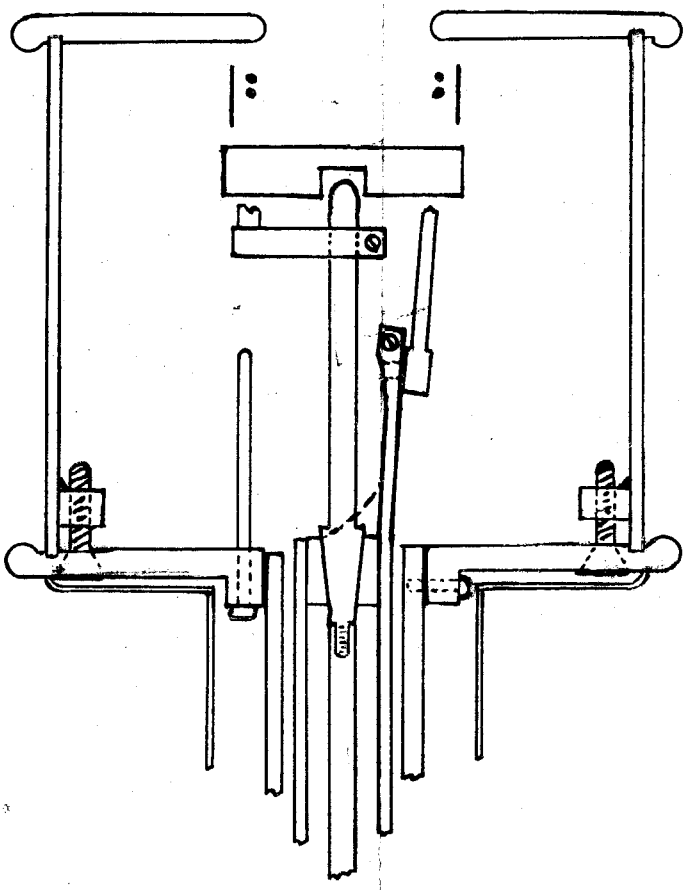

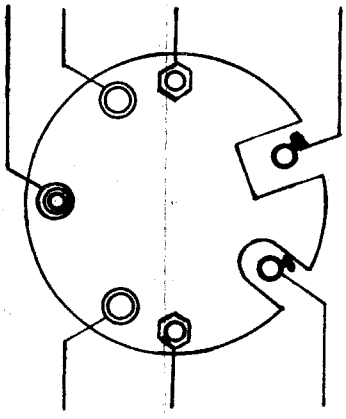

Fig. XIV

released from the cathode by positive ion impact. The origin purpose of the design of the indirect cathode was a study of this effect. However, Ohlin's data show that even at a pressure as high as 8×10^{-5} mm of Hg the mean energy of the secondaries is about 2 Volts or 1/10,000 of our voltage. Since our operating pressure was always 2×10^{-5} mm or lower it was felt that a further investigation of the effect of pressure on our result would be unnecessary. The conclusions as to the low energies of secondary electrons caused by positive ion bombardment is in agreement with direct studies of the energy distribution of these secondaries.(95 - 96)

Grave doubts can be raised as to whether the cause of the effect observed by Ohlin is really a matter of secondary electron emission. The main objections against such a view are 1) that Ohlin found the ion current much too small to account for the observed effect 2) that the "pressure effect" greatly raises the total observed intensity (the intensity is doubled at a pressure of 3×10^{-4} mm). The explanation which seems most likely is to attribute the observed effect to scattering of the soft X-rays by the gas in the spectrometer. In Ohlin's work the X-ray tube and the spectrometer were inter-connected; the "pressure effect" could therefore be due to decreased resolving power of the spectrometer owing to increased gas scattering. This explanation would account both for the increased intensity and the blurring of the limit.

The remainder of the X-ray tube construction remains as originally described.(87) The gyrating target mechanism was not used during our later runs since the power was insufficient to make a moving target necessary and since it was found

that the variation in the electric field caused by the target gyration caused a fluctuation in the tube current.

5) Method of Voltage Measurements

Since the Voltage enters linearly into the expression $fa\ h/_e$, the errors in voltage measurement enter directly into the final determination. The performance of the voltage measuring devices is therefore of considerable importance.

The voltage measuring device consists of a high voltage "voltbox" arrangement which operates into a Wolff Feussner type potentiometer. The construction of the voltboxes or "stacks", as we shall call them, is described by Bailey[29] and DuMond and Youtz[87]. The stacks consist of 20 spun aluminum pans, each containing 5 1 megohm resistance units. The resistance units are manufactured by the Shollcross company and wound of enameled nichrome wire of temperature coefficient .013 $^{o}C^{-1}$. The pans and the resistors are are assembled with lucite insulators. The lower resistance part of the voltbox is a single 500 Ω coil also wound with nichrome. There are two of these stacks, each assembled within a micarta column; taps are brought out through lucite bushings at several places in the high resistance unit. The wiring diagram of the two stacks is shown in Fig. XV. The resistance units are oil immersed; the oil can be circulated by means of a motordriven gear pump.

The performance of these stacks was not entirely satisfactory. By the method of calibration of these units, described later, it was found that the resistance ratios

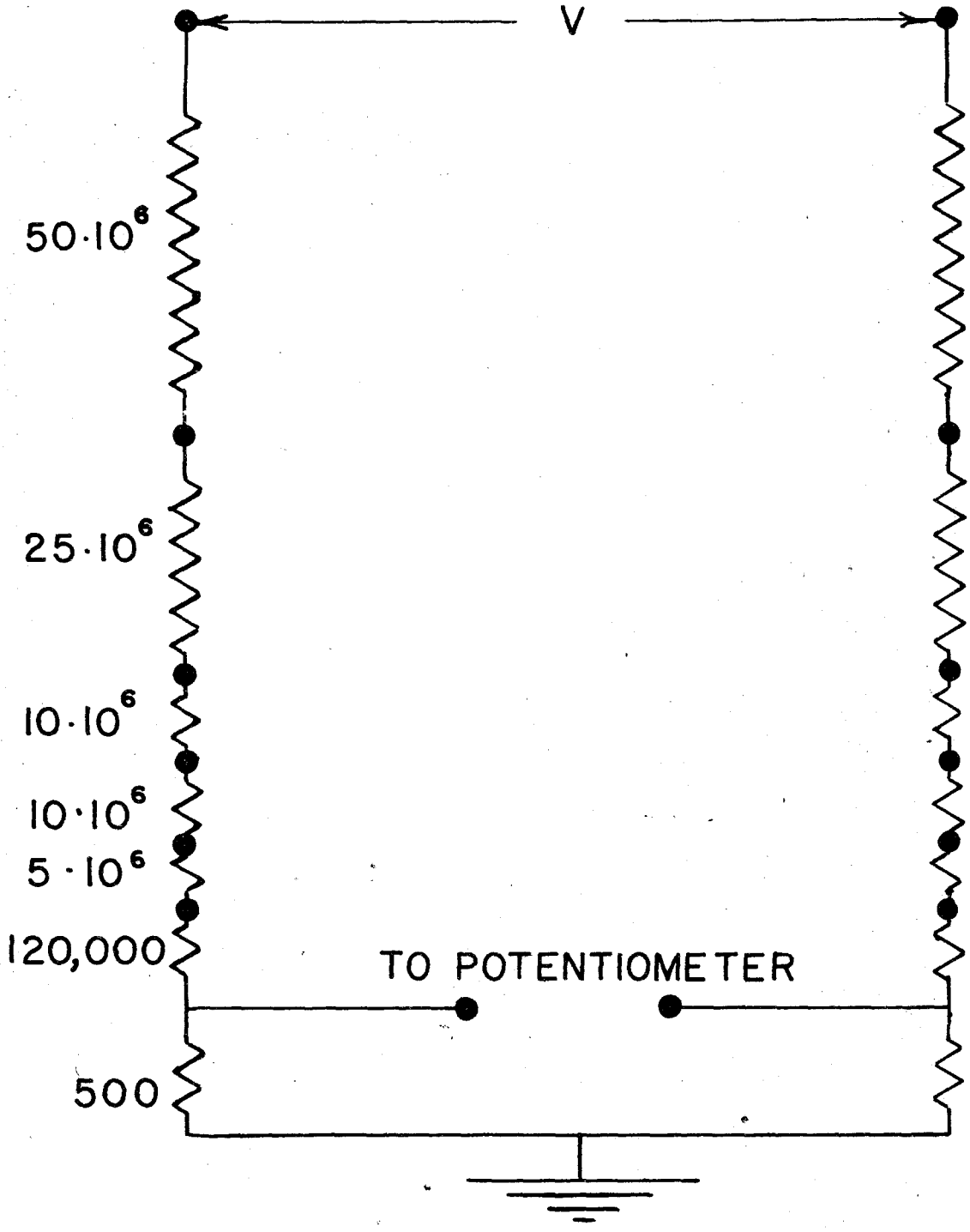

Fig. x_V

would change by as much as 8 parts in 10^4 during the course of a week. It was also found that the stacks had a negative loadcoefficient; i.e. the resistance ratio decreased with an increase in load across the stack. This load coefficient is of opposite sign to that which would be expected from the temperature coefficient of the resistance wires: since the expenditure of power per resistance unit is greater in the $10^6\Omega$ units than in the $500\,\Omega$ units and since the temperature coefficient of the wire is positive one would expect an increase of the dividing ratio with increased voltage across the stacks. The opposite sign of the load coefficient, therefore, indicates that the load coefficient is caused by some form of non-ohmic leakage. A careful refiltration of the transformer oil decreased the load coefficient considerably; its present value is less than 10^{-4} per 10 kilovolts.

The voltmeter is connected into the circuit as shown in Fig. VI. The voltages measured by the two stacks are very unequal: One stack measures nearly the entire tube voltage while the other measures only the drop across the regulator which is about 400 Volts on the average. It can be shown by a simple circuit analysis that under these conditions the stacks will have to be of equal ratio in order to make the drop across the potentiometer truly proportional to the X-ray tube voltage. The error introduced by an inequality of the two ratios causes an error of magnitude:

Fractional error in voltage = fractional deviation from equality of the two stacks × fractional inequality of voltages measured by the two stacks.

The fractional difference between the left hand and right hand stack ratios was never more than 8×10^{-4}; hence the error introduced by this inequality is less than $400/20,000 \times 8 \times 10^{-4} = 1.6 \times 10^{-5}$, and is therefore negligable.

The voltmeter was standardized against a group of 3 Weston Standard cells in a thermostatically controlled box; these cells had been checked by the National Bureau of Standards about 1 year ago and were also checked against three new cells loaned to us by the Department of Chemistry which had been certified very recently. The potentiometer had been originally calibrated by F. G. Dunnington and was recalibrated at the Bureau of Standards for this work. The two calibrations agree to better than 1 part in 10^{-4}.

Ripple measurements were made by placing an oscilloscope in series with a $.2\mu F$, 50,000 V condenser directly across the X-ray tube. This necessitated feeding the oscilloscope through an insulation transformer, since neither end of the tube is of ground potential. The oscilloscope was calibrated using an audio oscillator set at 150 cycles and a Weston rectifier type a.c. Voltmeter. The audio oscillator was placed directly across the X-ray tube.

6) The Monochromator

In most former investigations of the shortwavelength limit of the continuous spectrum the resolving power of the experimental arrangement had been limited by incomplete monochromatization of the X-ray beam. This width of the wavelength band passed by the monochromator was in general

determined by the required intensity. In this experiment it was attempted to make use of the large available primary intensity for purposes of permitting a narrower wavelength band.

Monochromatization of the X-ray beam was effected in two stages: First, a narrow wavelength band is selected by means of a double crystal spectrometer; the shape of the resultant band is then further modified by means of a set of balanced filters.

The two crystal spectrometers used in this work is the one designed and constructed by DuMond and Marlow.[97] The two crystals are mounted on rotating tables driven by a precision worm and gear drive. The whole spectrometer can be swung about the axis of the first crystal while the arm designed to carry the ionchamber can be swung about the axis of the second crystal. The drives for the four degrees of freedom (rotation of the two crystals, motion of the ion chamber arm and motion of the entire spectrometer) can be coupled with gears such that the condition of specular reflection is satisfied at both crystals for the same angle and such that the X-ray beam passes through the center of the ion chamber window for all settings of the spectrometer. The motion of the two crystals can be controlled to a fraction of a second of arc. All isochromat settings were near the line used for calibration; hence no correction for the gear-error had to be applied.

The reference line chosen for this work was the Ag $K\alpha_1$ line. Its wavelength has been carefully investigated by many

observers. The more reliable observations are

Observer	XU (Sieghahn)	year
Kellstrom	(98) 558.268	1927
Cooksey & Cooksey	(99) 558.237	1930
Bearden	(100) 558.255	1933
V Zeipel	(101) 558.225	1935
Berger	(102) 558.223	1936
Ingelstam	(103) 558.241	1936
Elg	(104) 558.231	1937

These values do not differ by more than 6×10^{-5} from one another. In our calculation we have adopted the value of Elg[104].

The two crystals were cleaved out of a single block. Their surfaces remained untreated. They were mounted and adjusted according to the method of DuMond and Hoyt[105]. In order to test the quality of the crystals, a rocking curve of intensity vs. angular position of one crystal was obtained in the parallel position of the spectrometer. The resultant curve had full width of 10.5" at half maximum. For our later settings of about 5° this represents a fractional width of about 5×10^{-4}.

For calibration purposes the Ag $K\alpha_1$ line was mapped out a considerable number of times; in particular the position of this line was checked before and after every run. A representative curve is shown in Fig. XVI. For purposes of calibration a spot 1/8" in diameter in the center of the target was silverplated. All that is necessary for calibration, then, is to center the (ordinarily eccentric) target and "explore" the line at reduced power input.

One of the primary considerations in the use of a two crystal spectrometer is the reduction of background from

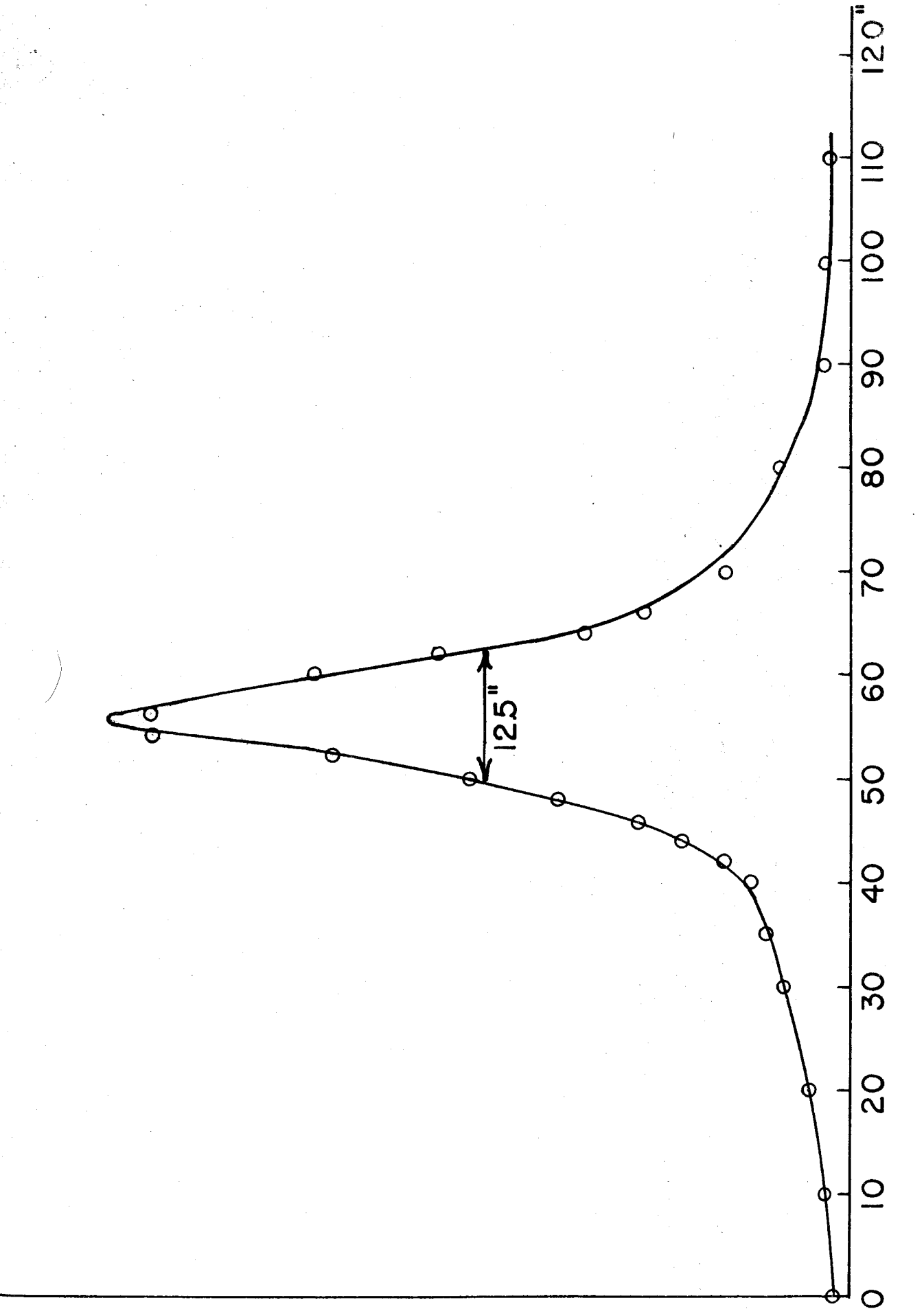

Fig. XVI

scattered radiation. After various attempts of placing lead slits and stops by ordinary geometrical considerations it was decided to explore the scattering photographically. It was found that a considerable amount of diffuse scattering takes place on the front surfaces of the crystals themselves. Fig. XVII shows an exposure of a film placed between the final crystal and the ion chamber; the film is placed about 1 cm from the edge of the crystal, the exposure is 10 min. at 25 KV, 100 ma. The film shows a very pronounced black edge which is a direct replica of the front surface of the crystal. The exposure was unsufficient to show the beam diffracted by ordinary Bragg diffraction. A two crystal spectrometer does not only select a practically monochromatic beam from the X-ray output of the tube but it also selects a beam practically homogeneous as to direction. The angular spread of the monochromatized beam can only be a few seconds of arc. However, a diffusely scattered radiation process can take place both over a wide range of angles and over a wide range of wavelengths. For this reason extreme precautions are required to keep the intensity of diffuse scattering below the intensity of Bragg diffraction. Other pictures showed the necessity of placing slits in front of several of the lead tunnels used for shielding in order to prevent small angle scattering from the walls of the tunnels. As a result of this photographic survey the slits and stops were arranged as shown in Fig. XVIII. Note in particular the thin stop directly behind the last crystal positioned such as to block tangential radiation from the crystal surface. As a result of these rearrangements, the intensity was considerably improved; practically all the scattering was effectively

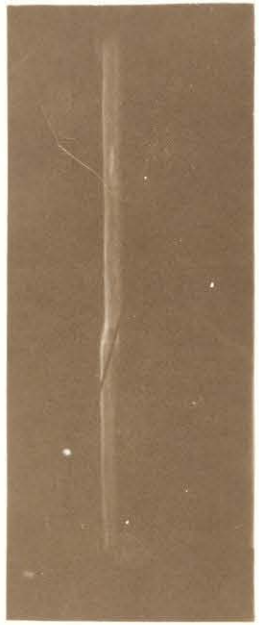

Fig. XVIII

XIX ?

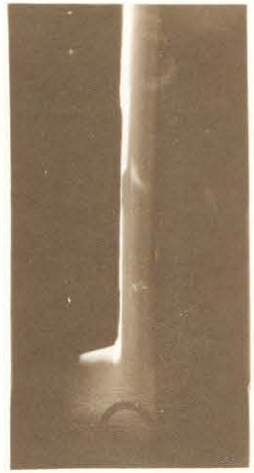

Fig. XVII

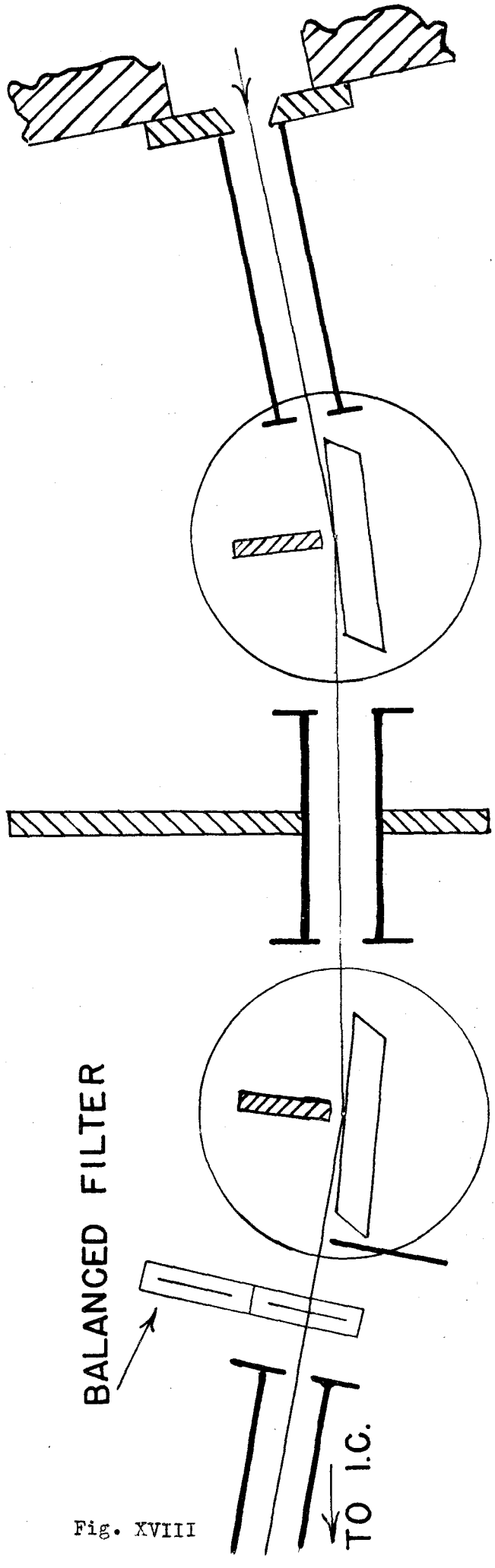

Fig. XVIII

suppressed as is shown by Fig. XIX; this photograph was taken by placing a photographic film directly in front of the ion-chamber window. Note the complete absence of scattered radiation. The width of the line shown in this figure is the width of the projected focal spot. The exposure required here was 1 hr at 100 ma tube current at 30 K V.

As is shown by the small width of the parallel position rocking curve and also by the small width of the Ag K_{α_1} profile, the resolving power has been very greatly improved as compared with former work. Nevertheless it was feared that the effect of the combination of the slowly decaying "wings" of the crystal diffraction pattern in combination with the ramaining incoherent scattering would give rise to a considerable blurring of the short wavelength limit. For this reason the action of the two crystal spectrometer was supplemented by a pair of balanced Ross[106] filters. The action of balanced filters is as follows: Let in Fig. XX A represent the intensity absorbed by a metal of a certain atomic number and B be the intensity absorbed by a metallic foil of higher atomic number. Let the thickness of the two foils be so adjusted that the total absorption of the foils on the long wavelength side shall be equal. If this condition is fulfilled, then the only change in transmitted intensity when one of the foils is substituted in the beam for the other will be due to radiation contained within the wavelength band embraced between the two K absorption edges of the two metals; in addition to this some change in intensity will take place due to the fact that if the filters are perfectly "balanced" on the long wavelength side, the balance will necessarily be slightly

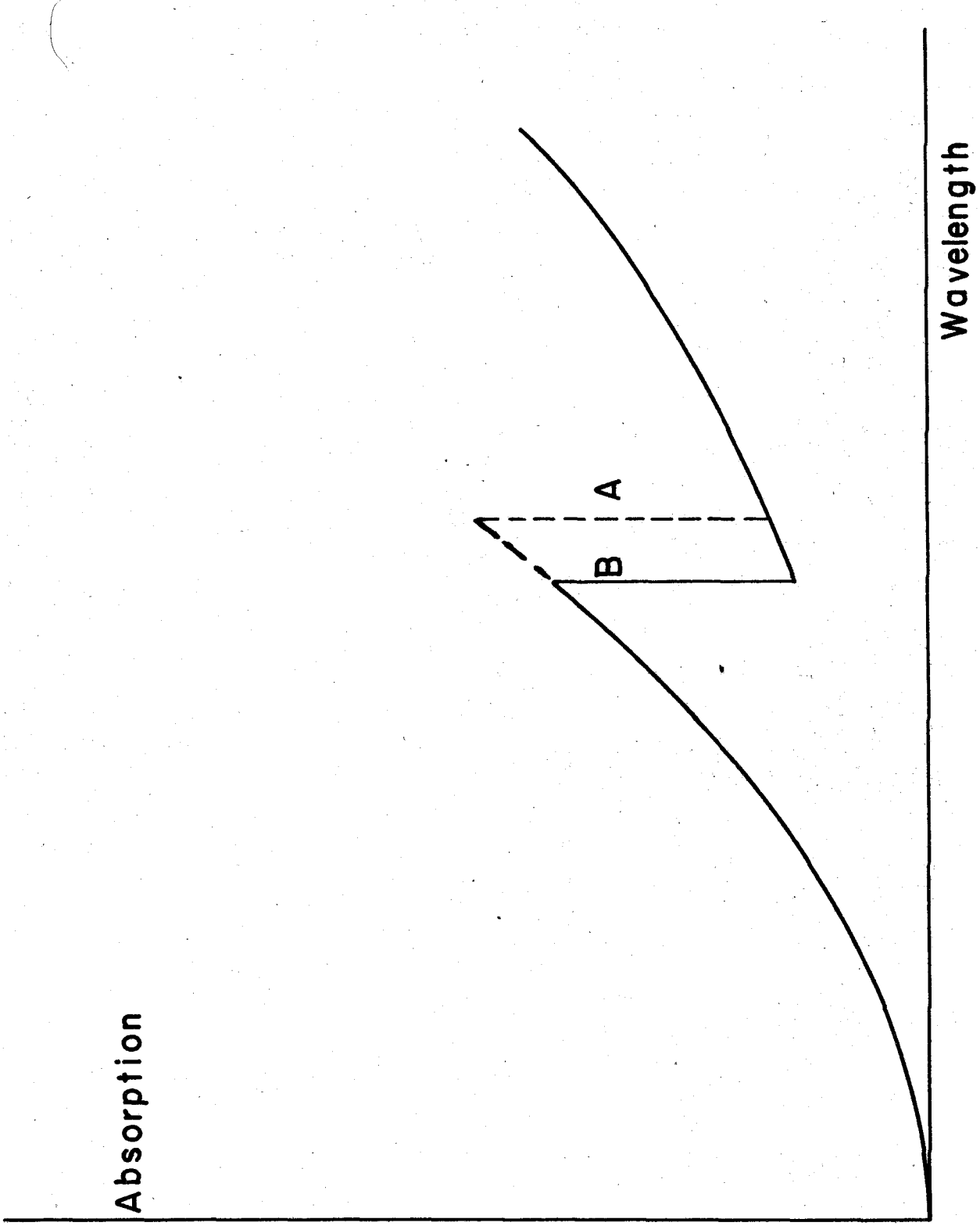

Fig. XX

imperfect on the short wavelength side of the K-edges.

Now consider the effect when the filters and the spectrometer settings are chosen such that the two crystal spectrometer pass band falls close to the longer one of the two K edges, but is inside the wavelength interval between the two edges. If now difference readings obtained on substitution of one filter in place of the other are taken, then any effect of the radiation, whose wavelength is longer than the critical wavelength of the K edge of the metal of lower atomic number, will be eliminated in the difference. The imperfect balance on the short wavelength side is in this case immaterial since there is no radiation present which is shorter than the limit. If the "fillet" of the observed isochromat is due to the causes mentioned above, then the use of a set of balanced filters in place of the customary lead shutter would be a decided advantage.

Several sets of balanced filters were kindly loaned to us by Prof. Paul Kirkpatrick. The set used in the isochromats in the neighbourhood of 20 kV contained Palladium and Molybdenum foils with the latter metal providing the "critical" edge. The filters were balanced on the long wavelength side by setting the pass band of the two-crystal spectrometer by a few minutes of arc on the long wavelength side of the Mo K edge wavelength; the filters in the X-ray beam was then adjusted until no appreciable difference in ion current was observed when the filters were exchanged. The filters are about 1" x 2 1/2" and are mounted in small brass frames. The frames are suspended from a crossbar with a milled rectangular groove; this crossbar rolls on two 1/2" steel balls which in

turn move in rectangular slots milled in stands waxed to the spectrometer top. The third point of contact is provided by another steel ball which is soldered into a cross arm connecting the two stands. The two filters are pulled back and forth by a string leading to the control desk and a spring, respectively. This method of mounting produces a very reproducable motion of the filters, which is essential particularly if the foils are not very uniform. The effectiveness of the filters in reduction of background will be discussed later. The loss in intensity due to the filters is slightly in excess of a factor of two.

The vertical divergence angle in these experiments is about 1/20 radian; this allows a wavelength deviation of about .1% percent from the set wavelength[105]. The effect of the wide vertical divergence will be an asymmetrical "window curve" of the spectrometer; the maximum of the curve will, however, remain unshifted. The conclusions drawn as to the location of the short wavelength limit by means of the point of maximum curvature will therefore remain intact. The Ag $K\alpha_1$ line standardization curves are obtained at identical vertical divergence as the isochromats; hence any shift due to asymmetry ought to cancel.

7) The Ion Chamber and Ionization Current Amplifiers

The ion chamber used in connection with this work is of the same design as the one used by DuMond and Hoyt[105]. It is filled with Methyl bromide; its accelerating potential is supplied by an hexagonal wire grid removed about 3" from the wall of the chamber. The collector is a wire loop placed such as to be clear from direct X-ray impact. This

construction shields the "active region" from the effect of α- particles from the walls. As a further precaution the inside of the chamber was painted with a suspension of lampblack in clear lacquer. The collector lead leaves the bottom of the chamber through a quartz bushing. The ion chamber is screened on all sides with 2" of lead bricks (weighing 1250 lb total) to reduce the background. The background and leakage current is about 10^{-15} Amp and α - particle ionization bursts take place about once every 3 minutes.

The ionization current is measured by means of the standard Barth[107] circuit, as described by Penick[108]. The circuit is shown in Fig. XXI. The circuit was carefully balanced for a filament current of 270 ma; owing to changes in tube characteristics this balance could not be exactly maintained. The sensitivity of the amplifier, using a galvanometer of 6×10^{-10} Amp/mm sensitivity was 50,000 mm/Volt. The ionization currents were observed by means of the "steady deflection" method by using grid shunts. The resistance shunt most commonly used in these measurements has a value of 5×10^{11} Ohms, making the overall current sensitivity 4×10^{-17} Amp/mm and the time constant of the grid circuit about 10 sec. The sensitivity is easily sufficient to show individual pulses due to α - particles released inside the ionchamber; it is therefore unnecessary to average ionization readings due to α-particles into the results.

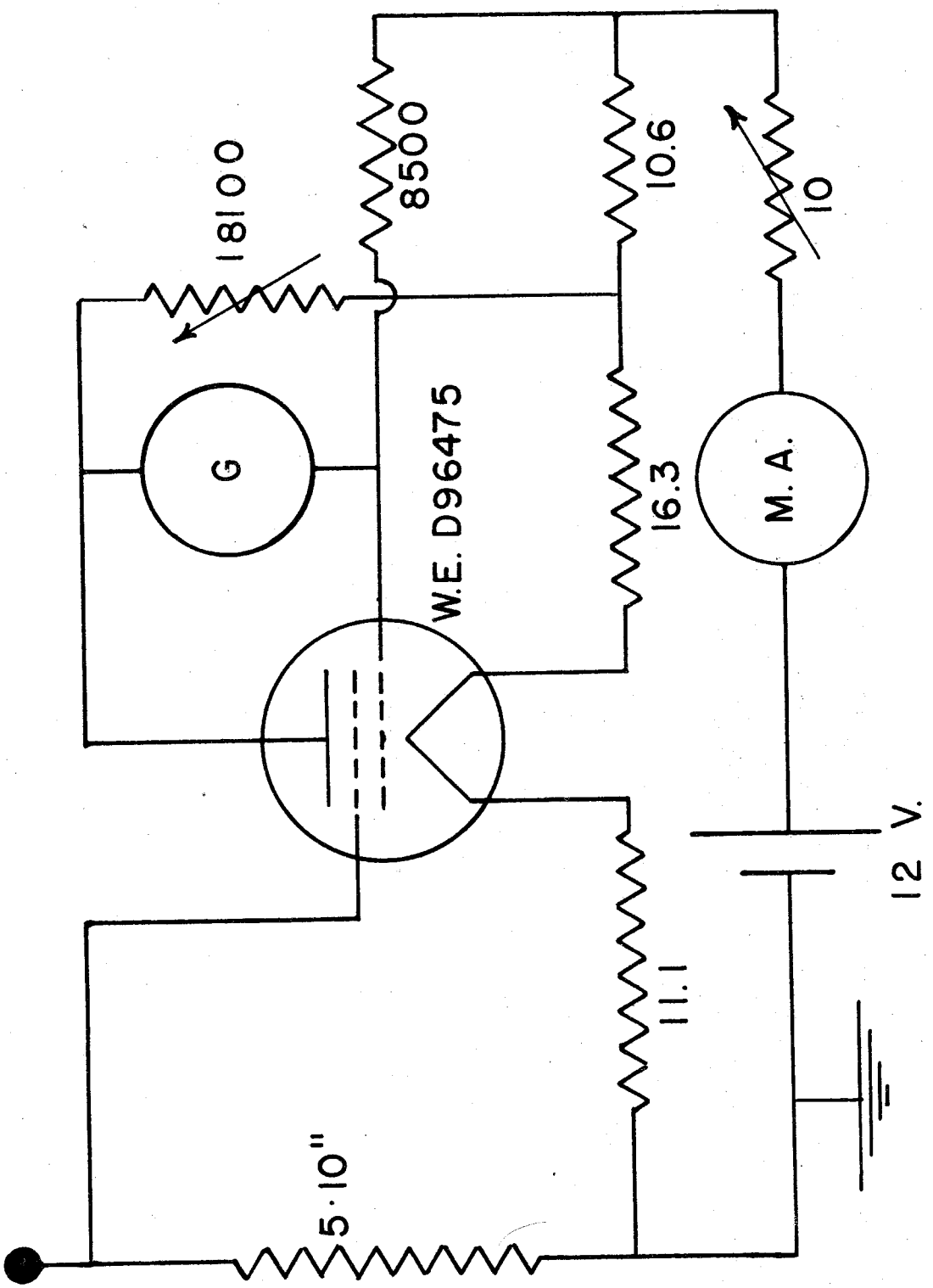

Fig. XXI

IV Experimental Procedure, Results, and Calculations.

An observation of an isochromat consists of tube voltage measurement, emission current measurement, and ioncurrent observation as a function of balanced filter position. Due to the unreliability of the voltage dividers, these were calibrated every 2 point on the isochromats. Each point on an isochromat is the mean of about 10 different readings.

1) Method of Voltage Calibration.

The problem in obtaining an accurate calibration of the voltage divider is to establish an accurate 200,000:1 ratio which can be compared to the ratio of the divider. A considerable number of methods for establishing such a ratio were devised; we shall only describe the one used in the final measurements.

Through the kindness of Dr. Frank Wenner of the National Bureau of Standards we had available a 0 - $10^6 \Omega$ standard resistance box and a 0 - 10,000Ω standard resistance box, both made of well aged manganin coils by Otto Wolff, Berlin. Each of the boxes has terminals, permitting subdivision of the resistances into 10 parts. We constructed an oil bath for the $10^6 \Omega$ box which permitted oil to be circulated at the rate of about 10 gals/minute. The oil was forced through 40 bakelite tubes reaching into the inside of each of the coils composing the megohm standard. Since the coils are wound on brass forms very efficient cooling is thus effected. Other resistances used in this measurement were a 50,000Ω Leeds and Northrup standard and a set of 0-5000Ω manganin coils made by the Rubicon company.

The primary step in establishing a well known ratio of 1:200,000 approximately was the establishment of an accurate $1:10^4$ ratio. This was done according to the method described by Wenner[109] as originally devised by Lord Rayleigh.[110] A comparison was made of the total resistance of the $10^4\,\Omega$ box with the 10 units of $10^5\,\Omega$ of the $10^6\,\Omega$ box all connected in parallel. Then the 10 units of the $10^4\,\Omega$ box were connected in parallel and the units of the $10^6\,\Omega$ box were connected in series; thus the ratio of the two resistances becomes $1:10^4$

Let r_i = resistance of the i^{th} unit of the 0-10,000 Ω box

R_i = resistance of the i^{th} unit of the 0-10^6 Ω box

δ_{ri} = deviation of r_i from their mean

δR_i = deviation of R_i from their mean

$\bar{r}$ = mean value of r_i

$\bar{R}$ = mean value of R_i

r_S, r_p, R_S, R_p resistances of series or parallel combinations of r_i and R_i.

We have

$$r_S = \sum_{i=1}^{10} r_i = \bar{r} \sum_{i=1}^{10} (1 + \delta r_i) = 10\bar{r} \qquad (28)$$

$$R_S = 10\,\bar{R} \qquad (29)$$

$$\frac{1}{r_p} = \sum_{i=1}^{10} \frac{1}{r_i} = \frac{1}{\bar{r}} \sum_{i=1}^{10} \left\{ \frac{1}{1+\delta r_i} \right\} = \frac{1}{\bar{r}} \sum_{i=1}^{10} \left\{ 1 - \delta r_i + \frac{\delta r_i^2}{2} - - \right\}$$

$$= \frac{10}{\bar{r}} \left\{ 1 + \sum_{i=1}^{10} \frac{\delta r_i^2}{2} \cdot \frac{1}{10} \right\} \qquad (30)$$

$$\frac{1}{R_p} = \frac{10}{\bar{R}} \left\{ 1 + \frac{1}{10} \sum_{i=1}^{16} \frac{\delta R_i^2}{2} \right\} \qquad (31)$$

$$\frac{R_S}{r_p} = 100\,\frac{\bar{R}}{\bar{r}} \left\{ 1 + \frac{1}{10} \sum \frac{\delta r_i^2}{2} \right\} = 10^4\,\frac{R_p}{r_S} \left(1 + \frac{1}{10} \sum \frac{\delta r_i^2}{2} \right) \cdot \left(1 + \frac{1}{10} \sum \frac{\delta R_i^2}{2} \right) \qquad (32)$$

None of the δ_{ri} and δ_{Ri} are greater than 2×10^{-4}; hence we have

$$\frac{R_S}{r_p} \simeq 10^4 \frac{R_p}{r_S} \qquad (33)$$

to a precision of 1 part in ten million.

Relation (33) is of course true only if the series parallel-connections are made so that the lead and contact resistances are negligable. The error due to lead resistances is negligable in all cases excepting in the case of the parallel connection of the 0-10,000Ω box. For this box special connectors, kindly supplied by Dr. Wenner, were used, made of heavy gage copper sheet, the resistance of which can be neglected. Since R_p and r_s are nearly equal, the ratio R_p/r_s in eq. 33 can be measured to high precision using an equal arm Wheatstone bridge. Such a bridge was constructed, using two of the 5000Ω Rubicon resistors as two of the branches and using R_p and r_s as the other two branches. Balance was obtained using a Kohlrausch slide wire in one branch (Fig. XXII). R_p and r_s were compared by interchanging them in the circuit and using the slidewire difference reading. Results could be read to 1 in 10^7. This fundamental ratio was found to be constant to 1 in 10^5 during its entire time in our hands. Precautions were taken regarding cross-leakage by mounting the resistances on paraffin. The other resistors used in the calibration of the voltmeter were then determined in terms of either the 10^4Ω or the 10^6Ω standard by preparing suitable equal arm bridges. The 5000Ω resistors were measured in terms of coils 1 to 5 of the 10,000Ω box; the 50,000Ω unit was measured in terms of coils 3-10 of the

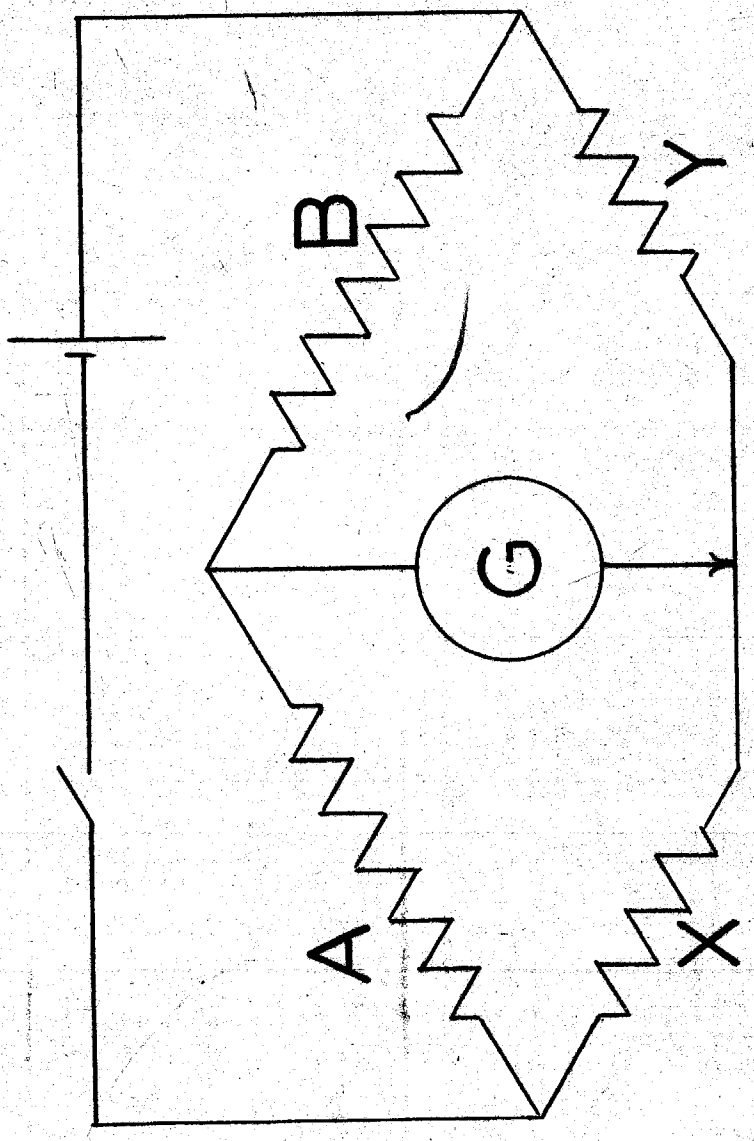

Fig. XXII

$10^6\Omega$ box connected in series parallel. All coils of the resistance boxes were interchecked. All box measurements could be made to a precision 1 in. 10^6; the changes in resistance of the coils,was, however, often more than this.

For purposes of calibration of the voltage stacks the resistors were connected as shown in Fig. XXI. The galvanometer deflection was reduced to zero by adjusting the Resistance R_x to a suitable value. The balance equation is:

$$\frac{A + B + R_x}{B} = \frac{R_1 + \rho_1}{\rho_1} \cdot \frac{\rho_3 + \rho_2}{\rho_3} \tag{34}$$

where

$$\rho_2 = \frac{R_3 R_4}{R_3 + R_4} \tag{35}$$

$$\rho_3 = \frac{R_5 R_6}{R_5 + R_6} \tag{36}$$

$$\rho_1 = \frac{R_2 (\rho_2 + \rho_3)}{R_2 + \rho_2 + \rho_3} \tag{37}$$

The nominal values of the resistances chosen for the main calibration were

$R_1 = 10^6\,\Omega$ (N.B.S. box = R_S)

$R_2 = 10^2\,\Omega$ (N.B.S. box = r_p)

$R_3 = 50{,}000\,\Omega$

$R_5 = R_6 = 5000\,\Omega$

$R_4 = 10^6\,\Omega$

This makes

$$\frac{A + B}{B} = 200{,}000 \left\{1 + 4.471 \times 10^{-3}\right\}$$

if all resistances had their nominal values.

Since the resistances deviate from their nominal values,

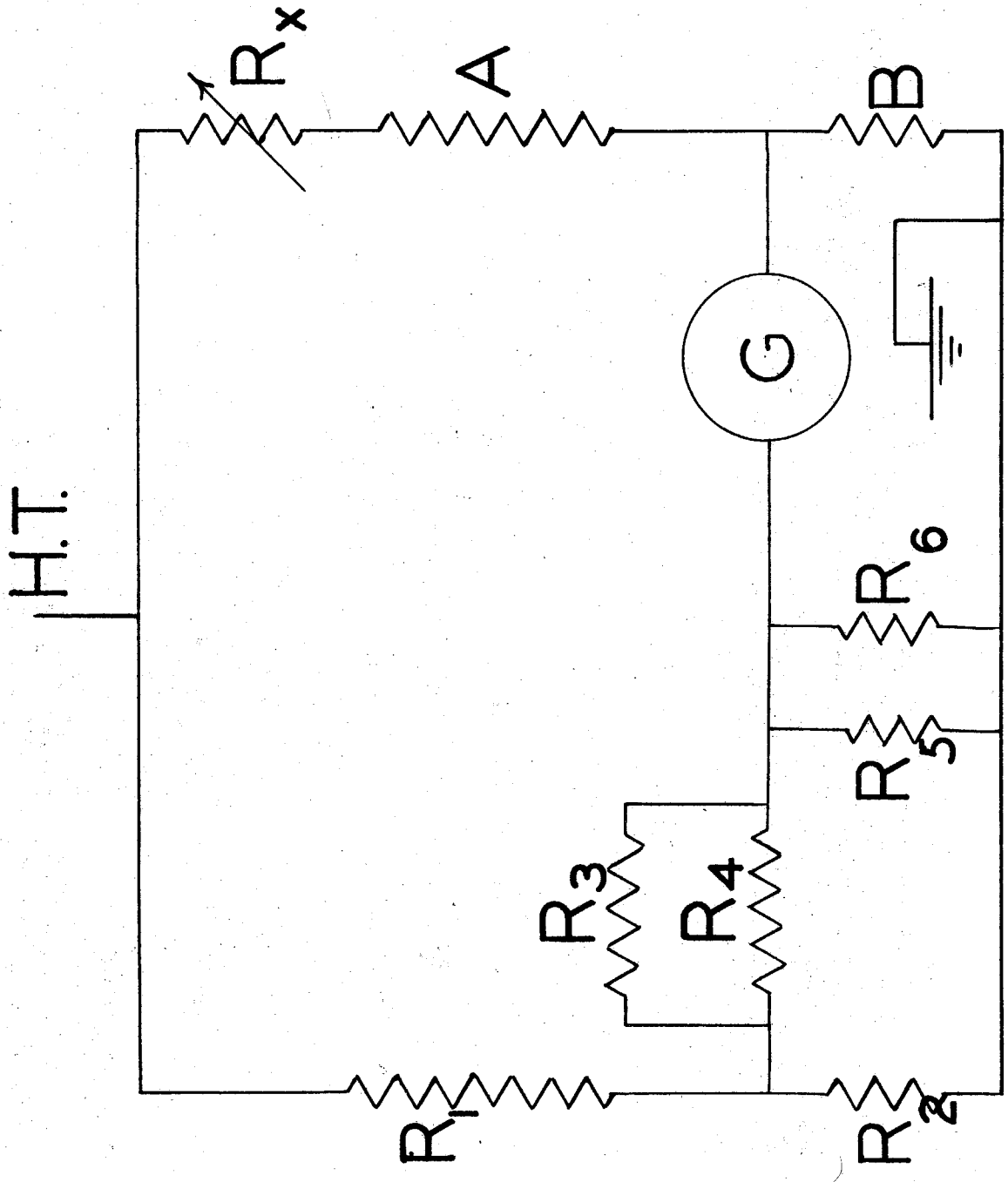

Fig. XXI

corrections must be applied to this nominal ratio. This correction is given by

$$\frac{\delta\left(\frac{A+B}{B}\right)}{\frac{A+B}{B}} = \frac{\delta\gamma}{\gamma} + \frac{\delta(\rho_3+\rho_2)}{\rho_3+\rho_2} - \frac{\delta\rho_3}{\rho_3} \qquad (38)$$

where $\gamma = \frac{R_1}{R_2}$, and where the δ quantities are the deviation from the nominal values of the quantities in question, as obtained by bridge measurement.

This method of calibration permits a calibration of the stacks to be executed with extreme rapidity, since all that is necessary to set up for calibration is to connect the $10^6\,\Omega$ box to the high voltage line and to connect the galvanometer to the appropriate places. Due to the allowable powerdissipation of the $10^6\,\Omega$ unit the calibration voltage is limited to 10 kV. It was ascertained beforehand that a rise from 25°C to 30°C in the temperature of the oil surrounding the $10^6\,\Omega$ unit would change the resistance of the unit by 2 parts in 10^5 only; in the calibration runs the temperature was always kept below 30°C.

Since the calibration could only be performed with 10 kV across the whole stack, its behavior at 20 kV was inferred by making a calibration of the two halves of the stacks at voltages up to 10 kV; as far as loading is concerned a voltage of 10 kV across each of the 50 megohm units is equivalent to a voltage of 20 kV across the entire stack. The load coefficient thus determined introduces a correction of 1×10^{-4} due to the difference in calibration at 10 kV and 20 kV equivalent voltage across the whole stacks.

2) Wavelength Standardization

The peak of the Ag $K\alpha_1$ line was located as described; the Braggangle was then shifted by 30' 58" bringing the spectrometer pass band to nearly 3' away from the Mo K edge. After the measurements the Ag $K\alpha_1$ line was re-located. In the calculations the mean value of the two peaks was used. The shift was .015%.

3) Internal Target Cleaning

The target was cleaned about every 2 hours during a run. No systematic dependance of the position of the points on the cleaning was observed.

4) Results

The final curve obtained at a voltage in the neighbourhood of 20 kV is shown in Fig. XXIV. The upper curve is obtained using a lead shutter; the lower curve is obtained by the use of a set of balanced filters. The points are reduced to constant tube current. Using the auxiliary constants

$C = 2.9977_6 \times 10^{10}$ cm/sec

$d_1 = 3.02904 \times 10^{-8}$ Siegbahn cm

ratio of absolute to Siegbahn scale: 1.00203

P9 = ratio of absolute to international volts = 1.00034

a scale of h/e values is plotted below the voltage scale. The correction for filament drop and tantalum workfunction has been made. Also temperature corrections to the crystal spacing was made. It appears that both the point of maximum curvature of the lead shutter curve and the filter curve lie at a value of

$$h/e = 1.3786 \times 10^{-17} \text{ erg sec/esu.}$$

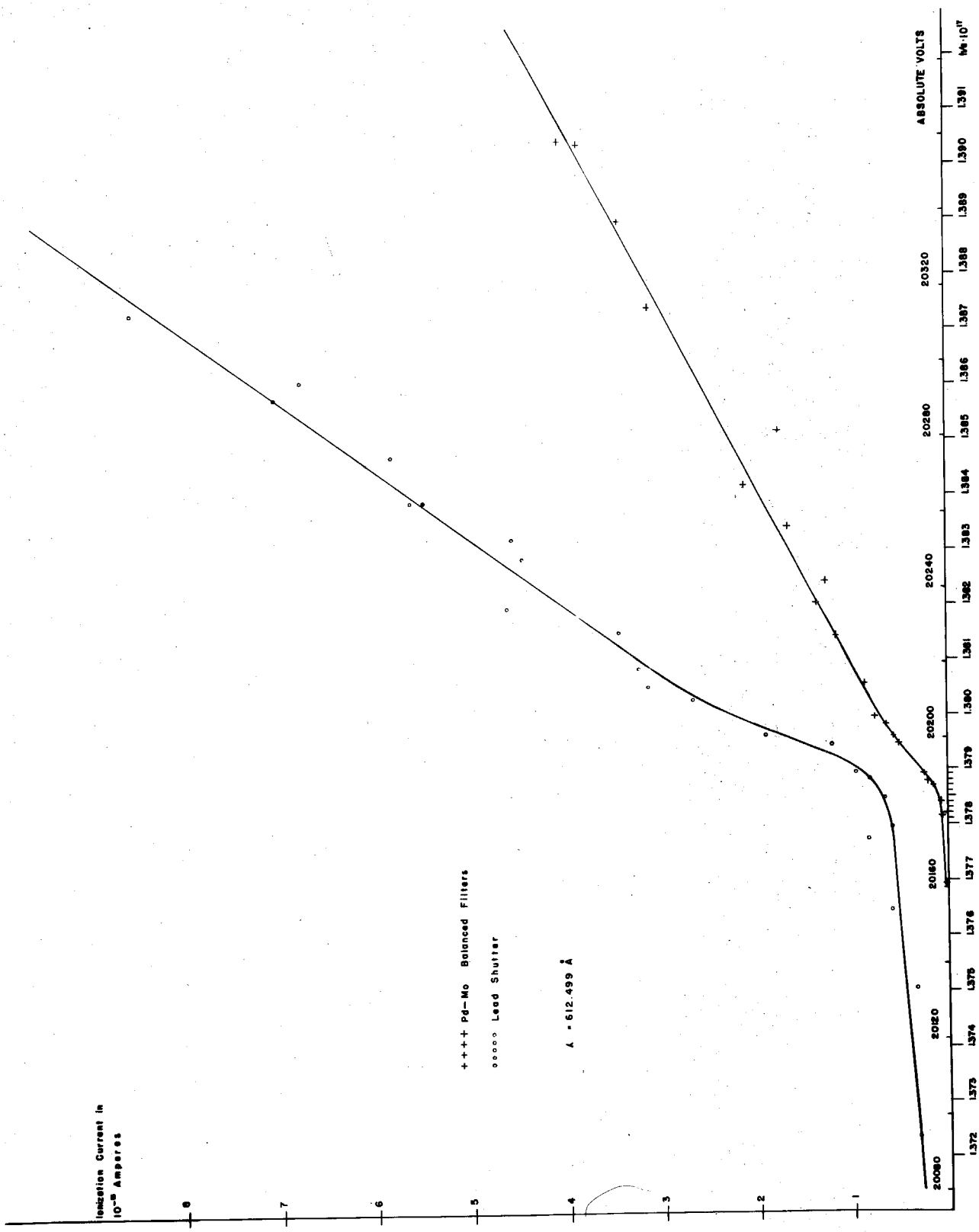
Ionization Current in
10^{-8} Amperes
++++ Pd—Mo Balanced Filters
ooooo Lead Shutter
λ - 612.499 Å
ABSOLUTE VOLTS
Mv·10¹⁷

Fig. XXIV

The difference in the sharpness of intercept between the two curves demonstrates the importance of the use of balanced filters for this work. The virtual coincidence of the points of maximum curvature as obtained by the two methods is, if not an experimental proof, at least experimental evidence for the analytic analysis of the behavior of an imperfect isochromat.

Using these experimental results we can now estimate roughly the value of the correction term

$$\sum_{i=1}^{\infty} g\,(z - X_i)\,(a_{i+1} - a_i)$$

of eq. (17) as compared to the principal term $g(z)\,f^1(0)$ of eq. (16). Let $g(z)$ be given by an equation of the form

$$g(z) = \frac{c}{1 + \frac{z^2}{a^2}} \qquad (39)$$

Let us assume that z be expressed on a scale using the intercept value of the voltage as unity. In our case the halfwidth a is "composed" (in the mathematical sense) of three terms

1) the halfwidth due to the crystal "window"
$a_1 = 5 \times 10^{-4}$ (expressed as fractional width)

2) the ripple voltage spread
$a_2 = 1.5 \times 10^{-4}$

3) the vertical divergence spread
$a_3 = 5 \times 10^{-4}$

4) the filament drop spread
$a_4 = 1.5 \times 10^{-4}$

Hence making the conservative assumption the a_i to be additive (which is true if all the causes of spread obey equation 39) we have

$$a = 13 \times 10^{-4}$$

The first appreciable change in slope takes place .15% above the

limit; hence

$$g\,(z - X_i) \simeq \frac{C}{1 + \left(\frac{z - 1.5 \quad 10^{-3}}{1.3 \times 10^{-3}}\right)^2}$$

while $$g(z) = \frac{C}{1 + \left(\frac{z}{1.3 \times 10^{-3}}\right)^2}$$

The change in slope at the first level is about -1/2 of the value of the slope at the intercept; the second derivative of the isochromat is therefore proportional to a quantity K given by:

$$K \simeq \frac{1}{1 + \left(\frac{z}{1.3 \cdot 10^{-3}}\right)^2} - 1/2 \left\{ \frac{1}{1 + \left(\frac{z - 1.5 \cdot 10^{-3}}{1.3 \cdot 10^{-3}}\right)^2} \right\} \qquad (40)$$

This curve is plotted in Fig. XXVI. It is seen that the maximum near $z = 0$ is displaced by a relative amount of 10^{-4}; the method of maximum curvatures is therefore applicable to this precision. The assumptions as to width of the $g(z)$ function and as to the mode of composition were quite conservative; hence the error due to this curve is probably less than 10^{-4}.

5) Discussion of Errors

Any estimate of error for an experiment of this kind must necessarily be based in part on the judgement of the experimenter as to the reliability of his apparatus and the magnitude of error introduced by scattering of data. Another difficulty which impairs the reliability of an error estimate is the fact that in some cases errors are estimated in terms of a "limit" of errors while in some cases the "probable" error is used. Of these terms only the "probable" error has a mathematical meaning in terms of

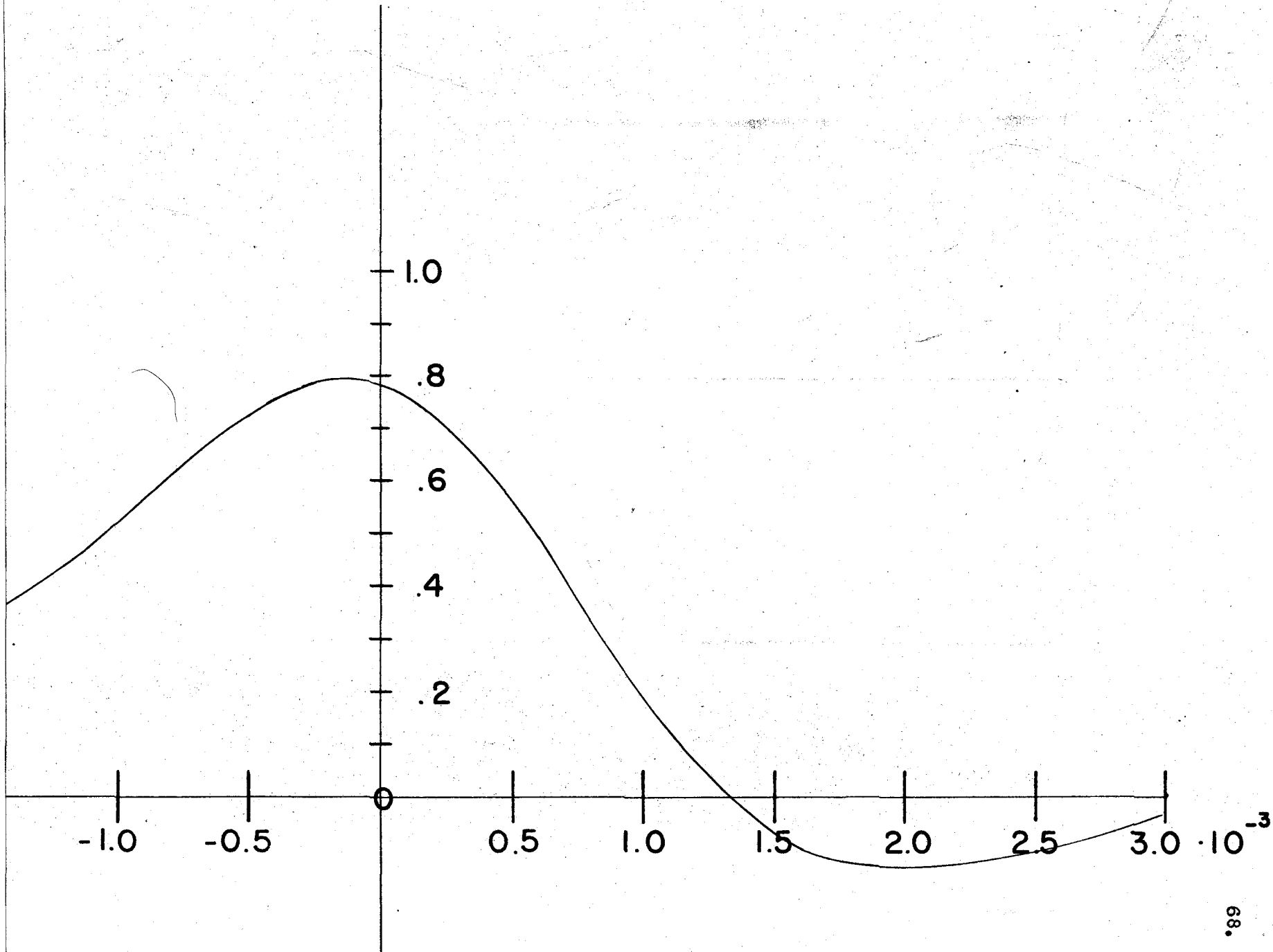
1.0
.8
.6
.4
.2
0
-1.0
-0.5
0.5
1.0
1.5
2.0
2.5
3.0 ·10^-3

any given distribution of data. The difficulty is that in many cases such a distribution is not available. For instance if we are dealing with a standard cell "certified" by the Bureau of Standards to .02% or a potentiometer "adjusted to .005%" we really have no way of obtaining a probable error in the mathematical sense. On the other hand if we are analyzing a set of scattered data, we cannot justify designating a certain value as a "limit" of error. From an experimental point of view one can simply multiply the probable error by an appropriate number and obtain an "experimental" limit. For instance, on the basis of a Gaussian error curve the chance of an error 3.5 times the probable error is only 1% which we may consider negligable. In listing the errors of this experiment both "limits" of error and "probable" errors are given; if only one or the other is known, the missing value is obtained by means of a conversion factor of 3.5.

	"Probable" error	"Limits" or error	in parts in
1) Standard cell	3	10	100,000
2) Potentiometer	6	20	
3) Voltmeter calibration	4	15	
4) Estimate of point of max. curvature	10	35	
5) Wavelength meas.	6	20	
Totals	14	100	

The totals are formed by direct addition in the case of the "Limits" of error and by geometrical addition in the case of the "Probable" errors. One result can therefore be quoted as

$$h/e = (1.3786 \pm .0002) \times 10^{-17} \text{ erg sec/esu}$$

on the basis of probable errors, and

$$h/e = (1.3786 \pm .0014) \times 10^{-17} \text{ erg sec/esu}$$

on the basis of limits of error. Note that after combination of errors by the method described above the probability of the error being the "limit" of error has become much less than 1%.

This result is shown in relation to other determinations of atomic constants in the DuMond isometric consistency chart Fig. XXVI. It is seen that the result is about six parts in 10,000 lower than the value computed indirectly by Birge[66], but is 7 parts in 10,000 higher than the mean of Bearden's and Schwarz's value; it is, however, considerably higher than the other older values. This experiment therefore does not confirm the existence of a serious discrepancy; the agreement is, however, not satisfactory enough as to make further investigations on the subject unnecessary.

Further work contemplated on this subject, cut short by the war, was the study of isochromats at higher voltages, the study of line excitation voltages as compared to absorption edges and to X-ray series limits. Such work, though not feasable at present, will undoubtedly be very desirable before the question as to the values of the natural constants can be considered as settled.

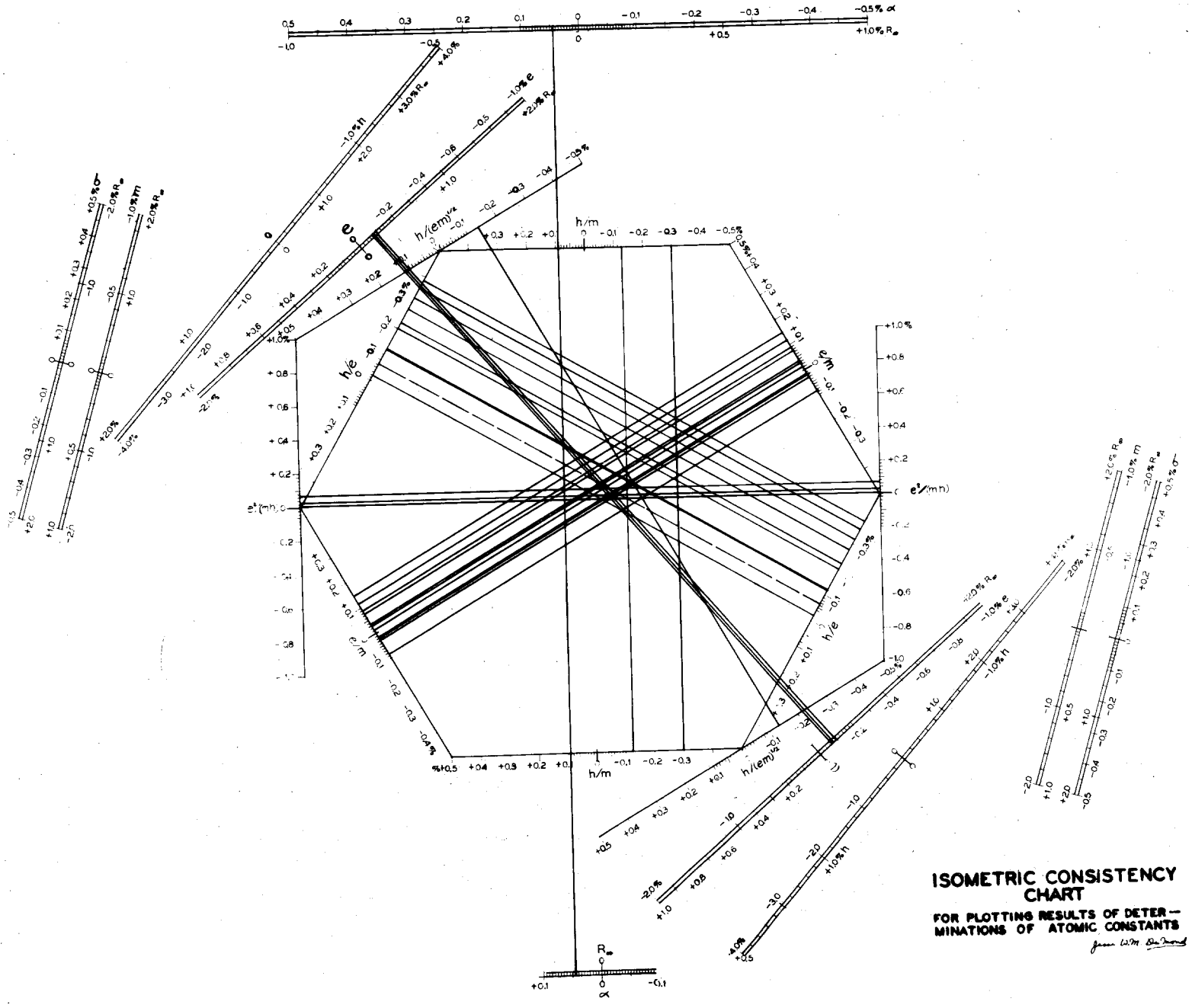
ISOMETRIC CONSISTENCY CHART
FOR PLOTTING RESULTS OF DETERMINATIONS OF ATOMIC CONSTANTS
James W. M. DuMond

Fig. XXVI

Acknowledgments

During the entire course of these experiments this work has been directed by Prof. J. W. M. DuMond. From him derives innumerable suggestions, valuable help and general inspiration without which this work would never have been possible. I express my deep gratitude for his kindness.

Several of the pieces of apparatus used in this investigation were kindly loaned to us by other men. The balanced filters were loaned to us by Prof. Paul Kirkpatrick of Stanford University. The resistance standards used in the voltage calibration were kindly loaned by Dr. Frank Wenner of the National Bureau of Standards. To him also I owe thanks for valuable advice regarding precision resistance measurements. Three standard cells used for interchecking our own three cells were generously loaned to us by Prof. Don Yost of the Dept. of Chemistry.

Work on this problem was begun under the direction of Dr. DuMond by Dr. H. H. Bailey. The work on the original Voltmeter assembly was done by him; work on the spectrometer, ion chamber and Filament supply was performed jointly. His valuable contributions are outlined in his thesis[29]. For the last year Mr. A. E. S. Green has taken an equal share in this investigation; in particular a considerable part of the voltage calibration work and taking of the data were done by him.

The complexity of the apparatus requires that at least two operators take part in every set of observations. For valuable assistance in this respect I express my sincere thanks to Mr. William Thompson Jr, Miss Evelyn Green, and Miss Adéle DuMond.

References

1) E. Bäcklin, Zeits. f. Physik 93, 450 (1935)

2) J. Bearden, Phys. Rev. 37, 1210 (1931)

3) J. Bearden, Phys. Rev. 47, 883 (1935)

4) J. Bearden, Phys. Rev. 48, 385 (1935)

5) M. Söderman , Nature 135, 67 (1935)

6) F. Tyrén, Nova Acta Reg. Soc. Scient. Ups. IV, 12 #1 1940

7) R.A. Millikan, Electrons (+ and -) Chicago (1934)

8) Bäcklin and Flemberg, Nature, 127 , 655, (1936)

9) Isbida, Fukushina and Suetsuga, Phys. Chem. Res. Tokyo 32, 57 (1937)

V. D. Hopper and T. H. Laby, Proc. Roy. Soc. A, 178 243 (1941)

10) F. Dunnington Phys. Rev. 52, 498 (1937)

11) F. Kirchner Ann. d. Physik 8, 975 (1931)

12) F. Kirchner Ann. d. Physik 12, 503 (1932)

13) A. E. Shaw Phys. Rev. 54, 193 (1938)

14) W. Houston Phys. Rev. 30, 608 (1927)

15) W. Houston Phys. Rev. 51, 446 (1937)

16) W. Houston Phys. Rev. 55, 423 (1939)

17) Shane & Spedding Phys. Rev. 47, 33 (1935)

18) R. C. Williams Phys. Rev. 54, 568 (1938)

19) Kinsler & Houston Phys. Rev. 45, 104 (1934)

20) Kinsler & Houston Phys. Rev. 45, 533 (1934)

21) J. A. Bearden Phys. Rev. 54, 698 (1938)

22) Duane, Palmer and Yeh J. Opt. Soc. Am. 5, 376 (1921)

23) P. Kirkpatrick and Ross Phys. Rev. 45, 454 (1934)

24) H. Feder Ann d. Physik 51, 497, (1929)

25) DuMond and Bollmann Phys. Rev. 51, 400 (1937)

26) Per Ohlin Dissertation, Uppsala (1941)

27) Per Ohlin Meddelande Fran Fysika Institutionen, Uppsala 12, 12- (1939)

Per Ohlin
28) Arkiv För Mat.Astro. och Fysik Vol 27B #10 (1940)

29) H. H. Bailey Thesis Pasadena (1941)

30) Bearden and Schwarz Bull. Am. Phys. Soc. May 1 - 3, (1941)

31) Schaitberger Ann d. Physik 24, 84 (1935)

32) H. T. Wensel J. Research N.B.S. 22, 386 (1939)

33) R. A. Millikan, Electrons (+ and -) Chicago(1934)

34) Lukinsky and Prilezaev Zeits. f. Physik 49, 238 (1928)

35) A. R. Olpin Phys. Rev. 36, 251 (1930)

36) E. O. Lawrence, Phys. Rev. 28, 947 (1926)

37) L. C. van Atta Phys. Rev. 38, 876 (1931)

38) L. C. van Atta Phys. Rev. 39, 1012 (1932)

39) Glockler Phys. Res. 27, 423 (1926)

40) Glockler Phys. Res. 33, 175 (1929)

41) Dymond Proc. Roy. Soc. 57, 291 (1925)

42) Dymond Phys. Res. 29, 433 (1927)

43) Mc Millen Phys. Rev. 36, 1034 (1920)

44) Löhner Ann. d. Phys. 22, 81 (1935)

45) Mohler, Bull. Nat. Res. Council IX p. 120 (1924)

46) Jones and Whiddington Phil Mag. 6, 889 (1928)

47) Roberts and Whiddington Proc. Leeds Phil. Soc. 2, 12 (1929)

48) Roberts and Whiddington Proc. Leeds Phil. Soc. 2, 46 (1930)

49) Taylor, Whiddington and Woodroofe , Proc. Leeds Phil. Soc. 2, 534 (1934)

50) Roberts and Whiddington Phil. Mag 12, 962 (1931)

51) Whiddington and Woodroofe Phil Mag 20, 1109 (1935)

52) Whiddington and Taylor Proc. Roy. Soc. A, 136, 651 (1932)

53) Whiddington and Taylor Proc. Roy. Soc. A, 145, 473 (1934)

54) Roberts, Whiddington and Woodroofe Proc. Roy. Soc. Sec. A 156, 270 (1936)

55) Lee and Whiddington Proc. Leeds Phil. Soc. 3, p 509 (1939)

56) S. van Friesen Dissertation Uppsala (1936)

57) S. van Friesen Proc. Roy. Soc. A150 424 (1937)

58) For a discussion of the value of R_∞ see

R. T. Birge Phys. Rev. 60, 766 (1941)

59) Kirkpatrick & Ross Phys. Rev. 45, 223 (1934)

60) Gnan Ann. d. Physik [5] 20, 361 (1934)

61) Christy and Keller Phys. Rev. 58, 658 (1940)

62) H. R. Robinson Phil. Mag. 22, 1129 (1936)

63) Clews and Robinson Proc. Roy. Soc. A 176, 28 (1940)

64) Kretschmar Phys. Rev. 43, 417 (1933)

65) R. T. Birge Reports on Progress in Physics London Physical Society. (In Print)

66) R. T. Birge Rev. of Modern Physics 13, 233 (1941)

67) J. W. M. DuMond Phys Rev. 56, 153 (1939)

68) J. W. M. DuMond Phys. Rev. 58, 457 (1940)

69) Dunnington Rev. Mod. Phys. 11, 72 (1939)

70) Kirchner, Die Atomaren Konstanten e, m, und h. Ergebnisse der exakten Naturwissenschaften (1939)

71) R. T. Birge Phys. Rev. 48, 918 (1935)

72) R. T. Birge Private communication. 11 - 27 - (1941)

73) Wehnelt & Jentsch Ann. d. Physik 28 , 537 (1909)

74) Schneider Ann. d. Physik 37, 569 (1912)

75) Cooke and Richardson Phil. Mag. 20, 173 (1910)

76) Cooke and Richardson Phil. Mag. 21, 404 (1911)

77) Cooke and Richardson Phil. Mag. 25, 624 (1913)

78) Cooke and Richardson Phil. Mag. 26, 472 (1913)

79) Lester Phil. Mag. 31, 197 (1916)

80) Wilson Proceedings Nat. Acad. Scien. 3, 426 (1917)

81) Wilson Phys. Rev. 24, 666 (1924)

82) Davisson & Germer Phys. Rev. 20, 300 (1922)

83) Davisson & Germer Phys. Rev. 24, 666 (1924)

84) Michel and Spanner Zeits. f. Physik 35, 395 (1928)

85) Duschman, Rowe, Ewald, Kidner Phys. Rev. 25, 338 (1925)

86) DuMond, Private Communication 3-9-1941

87) DuMond and Youtz, R.S.I. 8, 291, (1937)

88) Hunt and Hickman, R.S.I. 10, 6 (1939)

89) C. R. Barber R.S.I. 17, 245 (1940)

90) K.C.D. Hickman J. Frankl. Inst. 221, 215 & 383 (1936)

91) E. J. Williams Proc. Roy. Soc. A 130, 310 (1932)

92) E. Dushem R.S.I. 7, 86 (1936)

93) Pierce, Olson and Mac Millan R.S.I. 8, 145 (1937)

94) L. G. Parrat Phys. Rev. 54, 99 (1938)

95) L. Linford Phys. Rev. 47, 279 (1935)

96) Hill, Buechner, Clark, and Fisk Phys. Rev. 55, 463 (1939)

97) DuMond and Marlow R.S.I. 8, 112,(1937)

98) Kellström Zeits f. Phys. 41, 516 (1927)

99) C. D. Cooksey & D. Cooksey Phys. Rev. 36, 85 (1930)

100) J. A. Bearden Phys. Rev. 43, 92 (1933)

101) V. Zeipel Arkiv f. Mat, Astr. och Fysik 25A #8 (1935)

102) G. Berger, as quoted by Ingelstam(103)

103) Ingelstam Nova Acta Reg. Soc. Scien. Ups. IV 10 #5 (1936)

104) S. Elg. Zeits. f. Physik 106, 315 (1937)

105) DuMond and Hoyt Phys. Rev. 36, 1702 (1930)

106) P. A. Ross Journal Opt. Soc. Am. and R.S.I 16, 433 (1928)

107) Barth, Zeits. f. Physik 87, 399 (1934)

108) Penick, R.S.I. 6, 115 (1935)

109) Wenner, N.B.S. Journal of Research 25 RP 1323; p. 229 (1940)

110) Lord Rayleigh, Trans. Roy. Soc. 173, 697 (1882)

111) Perry and Chaffee, Phys. Rev. 36, 904, (1930)

112) D. V. Chu, Phys. Rev. 55, 475, (1939)

113) C. F. Robinson, Phys. Rev. 55, 423A,(1939)

114) Drinkwater, Sir Richardson, and Williams, Proc. Roy. Soc. A, 174, 104 (1940)

115) E. Gaedicke, Ann. d. Physik 5 36, 47 (1939)

116) R. T. Birge, A.consistent Set of Values of the General Physical Constants as of Aug. 1939. Privately circulated.